Nonlocal electroweak baryogenesis. II. The classical regime

Michael Joyce,* Tomislav Prokopec,† and Neil Turok‡
Joseph Henry Laboratories, Princeton University, Princeton, New Jersey 08544
(Received 18 October 1994)

We investigate baryogenesis at a first-order electroweak phase transition in the presence of a CP-violating condensate on the bubble walls, in the regime in which the bubble walls are "thick," in the sense that fermions interact with the plasma many times as the bubble wall passes. Such a condensate is present in multi-Higgs-doublet extensions of the standard model and may be formed via an instability in the minimal standard model. We concentrate on particles with typical thermal energies in the plasma, whose interactions with the wall are accurately described by the WKB approximation, in which a classical chiral force is evident. The deviations from thermal equilibrium produced by the motion of the wall are then treated using a classical Boltzmann equation which we solve in a fluid approximation. From the resulting equations we find two effects important for baryogenesis: (i) a classical chiral force term due to the CP-violating background and (ii) a term arising from hypercharge-violating interactions which are pushed out of equilibrium by the background field. Provided the wall propagates slower than the speed of sound, both terms lead to the diffusion of a chiral asymmetry in front of the wall. This can produce a baryon asymmetry of the observed magnitude for typical wall velocities and thicknesses.

PACS number(s): 98.80.Cq, 11.15.Ex, 11.30.Er, 12.60.Fr

I. INTRODUCTION

In this paper we present a detailed discussion of electroweak baryogenesis induced by a CP-violating condensate field on "thick" bubblewalls during a first-order electroweak phase transition. "Thick" in this context, and as we will see more precisely, means that the mean free time for a fermion propagating in the plasma is short compared to the time taken for the wall to pass. In this case one expects that the nonlocal quantum reflection effects, which such a CP-violating condensate has been previously shown to produce [1–3], will be suppressed because of scattering. Instead, we look for local classical effects, which can produce a driving force for baryogenesis. A classical treatment has, as we shall see, many advantages in that there is a systematic framework (a Boltzmann transport equation) within which to compute the nonequilibrium effects in which we are interested. A shorter version of this work has already appeared [4].

There is still considerable uncertainty as to what the relevant bubble wall thickness and speed are. Calculations are difficult [5] and strongly dependent upon the still poorly determined effective potential. A recent detailed study by one of us (T.P.) and Moore [5] using some of the methods developed in this paper indicates, within the minimal standard model, for Higgs-boson masses of order 30–70 GeV, and ignoring possible nonperturbative effects, a wall velocity ~ 0.4 and a wall thickness of order $\sim 25\ T^{-1}$, where T is the temperature. Thus, typically quarks interact very many times via gluon exchange processes as they cross the wall. If this is indeed the relevant regime, then for top quarks at least (the most obvious mediator of electroweak baryogenesis, since they couple most strongly to the bubble wall if one has standard model-like Yukawa couplings), the particle-wall problem cannot be treated without including the effects of strong (QCD) scattering from the plasma.

In an accompanying paper [6] we have introduced the essential ideas motivating the calculations that we undertake here. We showed there that the Lagrangian for a fermion propagating in the background of a bubble wall in a two-Higgs-doublet extension of the standard model can be written

$$\mathcal{L} = \bar{\Psi}\gamma^{\mu} i(\partial_{\mu} - i g_A \tilde{Z}_{\mu}\gamma^5)\Psi - m\bar{\Psi}\Psi\,, \tag{1}$$

where

$$g_A \tilde{Z}_{\mu} = g_A Z^{GI}_{\mu} - \tfrac{1}{2}[v_2^2/(v_1^2+v_2^2)]\partial_{\mu}\theta\,,$$

$$g_A = \pm\tfrac{1}{4}g,\quad g = \sqrt{g_1^2+g_2^2}$$

[6]. The + sign is for up-type quarks and (left-handed) neutrinos, and the − sign is for down-type quarks and charged leptons. g_1 and g_2 are the gauge couplings of the SU(2) and U(1) gauge fields; v_1 and v_2 the magnitudes of the vacuum expectation values (VEVs) of the two-Higgs-doublets, the first of which is taken to couple to the fermions through Yukawa terms. The two contributions to $\tilde{Z}_{\mu}$ come from the CP-odd scalar field θ, which is the relative phase of the two Higgs fields, $\varphi_2^{\dagger}\varphi_1 = Re^{i\theta}$, and the Z^{GI}_{μ} condensate discussed in [7], which may be present even in the minimal theory. All the vector couplings to $\tilde{Z}$ are removed by using the remaining unbroken

*Electronic address: joyce@nxth01.cern.ch
†Electronic address: tomislav@hepth.cornell.edu
‡Electronic address: neil@puhep1.princeton.edu

vector symmetries to remove the pure gauge $\tilde{Z}$ (the Z^{GI} condensate piece is also pure gauge if we treat the wall as planar and assume it has reached a stationary state in which the Higgs-boson and gauge fields are functions of $z - v_w t$). When the Higgs VEVs vanish, the axial $\tilde{Z}$ can be gauged away (for both fermions and Higgs-boson fields, with charges $g_A = 0$ and $g_A = -\frac{1}{2}g$ for the charged and neutral Higgs components, respectively, since $g_A = [\frac{1}{2}(T_3 - Y) + \frac{1}{4}(B - L)]g$ [6]).

However, on the bubble wall this pure gauge field has, as we shall see, very tangible CP-violating effects, even on particles with typical thermal energies. The axial gauge field condensate $\tilde{Z}$ formed on the bubble walls at the first-order phase transition violates CP spontaneously. $\tilde{Z}^0$ is odd under CP, and the spatial components $\tilde{Z}^i$ are CP even so that a bubble on which the spatial vector $\tilde{Z}^i$ points out everywhere is mapped under CP to one on which it points in. (Thus, in the latter case it is actually the gradient Z' that violates CP.)

The departure from thermal equilibrium, which this brings about as the bubble wall moves through the plasma, will source baryogenesis. In the comparison paper [6] we discussed the case originally investigated by Cohen, Kaplan, and Nelson (CKN) [1], when the fermion is treated as free on the bubble wall. The conditions for the validity of this treatment are discussed in [6] and roughly require that the wall thickness L be much less than the mean free path of the fermion λ_f. In this paper we consider the perturbations in the plasma produced by the CP-violating background in the possibly more realistic regime of wall thickness for which the fermions interact frequently on the bubble wall, a condition that will be specified more precisely in the course of our treatment.

As we have discussed in [6], one might expect that the inclusion of interactions would wipe out any interesting CP violation if the effect is a nonlocal quantum-mechanical one. This is precisely how the thin-wall limit has been understood [1–3]. However, as we noted in [6], the WKB limit is not as trivial as it appeared when viewed simply in terms of reflection coefficients for monotonic wall *Ansätze*. The fact that the dynamics of WKB particles are nontrivial and, in particular, that WKB particles propagate like particles in a classical CP-violating potential, suggests that there may be interesting effects that do survive when the scattering on the wall is included.

Second, as noted originally by CKN [8], such a CP-violating background perturbs the energy levels of particles and can push processes out of equilibrium locally. The original form of this "spontaneous" baryogenesis took this perturbation to the energy to be modeled by a fermionic hypercharge potential and calculated the resultant chemical-potential-driving baryon number violation by imposing constraints on exactly conserved quantum numbers. Both of these aspects of the calculation have been criticized. Dine and Thomas [9] pointed out that the fermionic hypercharge potential cannot be appropriate, as the effect does not vanish as the Higgs VEV vanishes. Subsequently, we pointed out [10] that the imposition of the constraints neglects transport processes, which tend to restore the region to a local thermal equilibrium in which there is no baryon number violation. The treatment we will present here will take account of both these criticisms and show that the essential effect does survive and can also, when transport is taken into account, source significant perturbations in front of the bubble wall [11]. This has also been pointed out in a recent paper by CKN [12]. One of the objectives of the present work is to bring these previously unconnected pieces into one coherent framework, which includes all the important effects and clarifies their relation to one another.

This paper is organized as follows. Section II discusses the WKB treatment of particle dynamics described by the Lagrangian (1). In Sec. III we introduce the Boltzmann equation and discuss the fluid approximation with which we truncate it to an analytically tractable form. In the following section we derive the resulting fluid equations. In Sec. V we analyze these equations in several steps, illustrating how perturbations may be generated in front of the wall and identifying the parameters that determine the behavior of the solutions. We derive the reduced equations needed for the calculation of baryon production in much of the favored parameter space of wall thicknesses and velocities. In Sec. VI we analyze these equations, treating the two source terms separately, and calculate the resulting baryon asymmetry in each case. In Sec. VII we compare the results we have found to those obtained in the thin-wall case in [6]. In Sec. VIII we conclude with a summary of the paper and a discussion of its shortcomings and directions for future work.

II. WKB DYNAMICS

The WKB approximation to the dynamics of particles in the background of the bubble wall is good provided the length scale on which this background varies is long in comparison to the de Broglie wavelength of the typical thermal particles we wish to describe. This is simply the requirement that the thickness of the bubble walls L be greater than T^{-1}. As we have indicated above, this is a very reasonable expectation.

To describe the WKB "particles," we turn to the Dirac equation derived from (1). The dispersion relation is obtained as follows. In the rest frame of the bubble wall we assume that the field $\tilde{Z}_\mu = (0, 0, 0, Z(z))$, and we can boost to a frame in which the momentum perpendicular to z is zero. In this frame the Dirac equation reads (after multiplying through by γ^0)

$$i\partial_0\psi = \gamma^0(-i\gamma^3\partial_z + m)\psi - g_A Z\Sigma^3\psi\,, \tag{2}$$

where $\Sigma^3 = \gamma^0\gamma^3$ is the spin operator. Setting $\psi \sim e^{-iEt+ip_z z}$, we see that the energy is given by the usual expression for a massive fermion plus a spin-dependent correction. The eigenspinors are just the usual free Dirac spinors. Returning to the $p_\perp \neq 0$ frame amounts to replacing E with $\sqrt{E^2 - p_\perp^2}$, from which we find the general dispersion relation in the wall frame:

$$E = [p_\perp^2 + (\sqrt{p_z^2 + m^2} \mp g_A Z)^2]^{1/2},\ \ \Sigma^3 = \pm 1\,, \tag{3}$$

where Σ^3 is proportional to the spin S_z as measured in the frame where $p_\perp$ vanishes. The same dispersion relation holds for antiparticles. The particles we are most interested in for baryogenesis are left-handed particles (e.g., t_L) and right-handed antiparticles ($\overline{t_L}$), since these couple to the chiral anomaly. Note that they couple *oppositely* to the Z field.

In Fig. 1 these dispersion relations are plotted for $p_\perp = 0$ for (i) $m > g_A Z$, (ii) $m < g_A Z$, and (iii) $m = 0$. We see how the branches deform into one another as we turn on the mass. In particular, we note how the left- (L-) and right- (R-) handed branches break up into two pieces and form the $\Sigma^3 = \pm 1$ branches, as the mass couples the two chiral components on the wall. Correspondingly it is straightforward to see how the eigenspinors (the usual Dirac massive eigenspinors) become chirality (γ^5) eigenstates for $p_z \gg m$. The conservation of spin on the wall gives a simple picture of how this happens—an in-going left-handed particle incident on the wall evolves in an eigenstate of spin on the wall. If its momentum is reversed it emerges as a right-handed particle, since its spin is conserved.

For what comes below, we will find it useful to keep this identification in mind. We label the states on the wall by the states they deform into as the mass is turned off and write the dispersion relation as

$$E^{L,R} = [p_\perp^2 + (\sqrt{p_z^2 + m^2} \pm \mathrm{sgn}(p_z) g_A Z)^2]^{1/2} \to [p_\perp^2 + (p_z \pm g_A Z)^2]^{1/2} \quad \text{as } m \to 0\,, \tag{4}$$

where the $+$ ($-$) singles out the states which become L (R) in the unbroken phase. (We assume the wall propagates from left to right, so that incident particles from the unbroken phase initially have $p_z < 0$.) The antiparticle $\bar{L}$ of a left-handed particle L is right-handed, and so we write the dispersion relation for antiparticles as

$$E^{\bar{L},\bar{R}} \equiv p_0^{\bar{L},\bar{R}} = \{p_\perp^2 + [\sqrt{p_z^2 + m^2} \mp \mathrm{sgn}(p_z) g_A Z]^2\}^{1/2}\,. \tag{5}$$

In the WKB approximation we take each particle to be a wave packet labeled by canonical energy and momentum ($E = p^0, \vec{p}$) and position $\vec{x}$. To compute the trajectory of such a wave packet, we first calculate the group velocity

$$v_i = \dot{x}_i = \partial_{p_i} E\,, \tag{6}$$

and second, using conservation of energy $\dot{E} = \dot{x}_i \partial_i E + \dot{p}_i \partial_{p_i} E = 0$, we find

$$\dot{p}_i = -\partial_i E\,. \tag{7}$$

Together these constitute Hamilton equations for the particle. The *momentum* of the particle is not a gauge-invariant quantity, but the particle worldline certainly is, and we can, for example, calculate the acceleration from the Hamilton equations. We find

$$\frac{dv_z}{dt} = -\frac{1}{2}\frac{\partial_z(m^2)}{E^2} \pm \frac{\partial_z(g_A Z m^2)}{E^2\sqrt{(E^2 - p_\perp^2)}} + O(Z^2)\,, \tag{8}$$

where of course E and $p_\perp$ are constants of motion. The first term describes the effect of the force caused by the particle mass turning on, and the second describes the chiral force. In the massless limit the latter vanishes, as it should because in this case the chiral gauge field can just be gauged away.

We shall later need a few more explicit expressions: namely,

$$v_\perp = \frac{p_\perp}{E}, \quad v_z = \frac{1}{E}\left(p_z \pm g_A Z \frac{|p_z|}{\sqrt{p_z^2 + m^2}}\right), \qquad \dot{p}_\perp = 0, \quad \dot{p}_z = \frac{\sqrt{p_z^2 + m^2} \pm \mathrm{sgn}(p_z) g_A Z}{E}\left(\pm \mathrm{sgn}(p_z) g_A \partial_z Z + \frac{\partial_z m^2}{2\sqrt{p_z^2 + m^2}}\right). \tag{9}$$

As $m \to 0$, we recover the equations of motion for the L and R particles in the pure gauge field Z.

Before we move on let us remark on our neglect of one effect in deriving these dispersion relations: thermal corrections to the fermion self-energies. In Appendix C we discuss how the dispersion relations and consequently the force terms are modified when one includes this effect. Depending on whether the Z field is "strong" or "weak" in the sense defined in the appendix, one can show that the resulting dispersion relations are either those given here plus small corrections or slightly modified ones that lead to force terms with altered momentum dependence. This is a complication we will ignore in the rest of this paper.

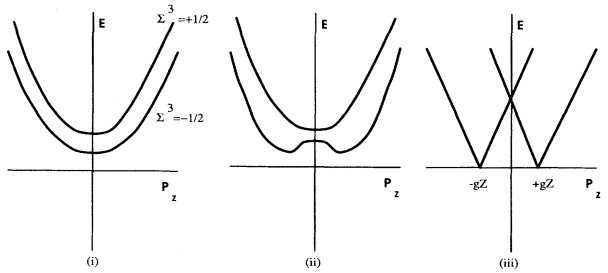

FIG. 1. Dispersion relation for particles in a background axially coupled pure gauge field. The plots show the energy E as a function of canonical momentum p_z for $p_\perp = 0$, for (i) $m > g_A Z$, (ii) $m < g_A Z$, and (iii) $m = 0$.

III. THE BOLTZMANN EQUATION IN THE FLUID LIMIT

Since most particles in the plasma are well described by the WKB approximation with respect to their interactions with the wall, we proceed to treat the fluid of such excitations as consisting of classical particles with definite canonical position and momenta and energy given by the derived dispersion relations. The Boltzmann equation for the phase space density $f(\vec{p},\vec{x},t)$ is

$$d_t f = \partial_t f + \dot{\vec{x}}\cdot\partial_{\vec{x}} f + \dot{\vec{p}}\cdot\partial_{\vec{p}} f = -C[f]\,. \tag{10}$$

The collision integral $C[f]$ describes how the phase-space densities are changed by interactions. The dominant interactions, which we will consider, are, because of Debye screening, short ranged and to a first approximation may be treated as pointlike. They are to be calculated at a given spatial point $\vec{x}$ using the Dirac spinors appropriate to the local value of the background fields $m(\vec{x})$, and $Z(\vec{x})$, taken to be constant. The Boltzmann equation is, in principle, solvable, but in order to make it analytically tractable we shall consider an approximation (truncation) that we expect to be quantitatively reasonable based on a perfect fluid form for the phase-space density. If interaction rates are fast, the collision integral forces the phase-space density towards a form that minimizes it, namely, local thermal equilibrium. For the case of a single fluid this means the form

$$f(\vec{p},\vec{x},t) = \frac{1}{e^{\beta(\gamma(E-\vec{v}\cdot\vec{p}))-\mu}\pm 1}\,, \tag{11}$$

where β, μ, and $\vec{v}$ are functions of $\vec{x}$ and t, and $\gamma = 1/(1-v^2)^{1/2}$. Imposing this form on the left-hand side of the Boltzmann equation and integrating to find the moments, one arrives at a set of coupled equations for the functions $\beta(\vec{x},t),\mu(\vec{x},t),\vec{v}(\vec{x},t)$, which parametrize the phase-space density. Expressed in terms of the energy density ρ, number density perturbation n, pressure p, and velocity $\vec{v}$, these become the familiar fluid equations in the case of a free fluid:

$$\begin{aligned}\partial_t n + \vec{\nabla}\cdot[\gamma n\vec{v}] &= 0\,,\\ \partial_t\rho + \vec{\nabla}\cdot[(p+\rho)\gamma\vec{v}] &= 0\,,\\ \partial_t[(p+\rho)\gamma\vec{v}] + \vec{\nabla}p &= 0\,.\end{aligned} \tag{12}$$

We are going to treat the approximately left-handed excitations L and their antiparticles $\bar{L}$ as two fluids, making an *Ansatz* of the form (11) for each.

This requires some justification because the dominant interactions, which bring our fluids to the form (11), are the same ones that damp away the temperature and velocity differences with respect to the background. This is not true of the chemical potentials, which are only attenuated by slower chirality changing processes. We keep the temperature fluctuation δT in order to quantify the rate at which the form (11) is approached. We use the velocity perturbation in the form (11) to model the anisotropic response to the force. We will, in fact, see that the precise form of this perturbation does not enter the final result, and its only role is to allow the particles to move in response to the force and set up a chemical potential perturbation.

In the present case we wish to determine how different species are perturbed by source terms, which will enter these equations in a way we will calculate. In particular, we must distinguish between particles and antiparticles, as it is the difference in the perturbations to these that is needed to source baryon production through sphaleron processes. To do this, we will treat each particle species as a fluid described by the fluid *Ansatz* (11) (in which the functions $\beta,\mu,\vec{v}$ are allowed to be different for each species), which makes the self-interaction collision terms zero. We then superimpose on this the interactions of these fluids, which will lead to terms in the equations damping all these perturbations to the local thermal equilibrium for the whole fluid.

Is this a good approximation? There are three conditions that must be satisfied.

(i) The interactions must be fast enough to ensure the system is maintained in the approximate form (11) as the wall moves. This should be a good approximation if the time the wall takes to pass is long in comparison to the time scale τ for the system to attenuate fluctuations away from this form; i.e., we want $L/v_w > \tau$. What should we take this time scale to be? We will see in due course that this question receives an answer within our calculation: We should take the scale τ to be approximately D, the diffusion length.

(ii) The rate at which the system is brought to this local equilibrium form should be faster than the rate at which the perturbations we keep in our *Ansatz* are attenuated. This is *not* the case because the same gluon exchange processes, which force f to the form (11), also damp away the velocity and temperature perturbations. Thus (11) is unlikely to be a very accurate description of the precise form of those perturbations. The chemical potential fluctuation will be the crucial term in our answer, which shall determine the final baryon asymmetry, and this is attenuated only by processes that change the number of particles in our "fluids." As we will discuss at length, these are indeed typically much slower than the gauge boson exchange processes, which damp δT and $\vec{v}$. The temperature perturbation shall actually play only a small role—we keep it merely to see how thermalization occurs and to estimate its rate.

(iii) The mean free time for particle interactions should be long compared to their energies, in order that we can describe the physics in terms of a set of "free particle" eigenstates of well-defined energy. This condition means the "width" of a state ΔE should be much smaller than its energy E. The particles of central interest in this paper have energies $E \geq T$, and $\Delta E \sim g^2 T$, so the condition is reasonably well satisfied even when one includes the strong interactions.

We should also mention a subtlety about the distribution (11). The form is dictated by the quantities that are conserved in the local interactions. That these are $E = p_0$ and $\vec{p}$ is a nontrivial fact in this case in which the gauge symmetry is broken. In the presence of a pure gauge field, it is not immediately obvious whether one

should take just the canonical momentum or perhaps some linear combination with the gauge field, as the correct conserved quantity.

For a conserved gauge charge, which one is chosen is immaterial, since the difference can always be absorbed in the chemical potential, which is determined by the condition on the conserved charge. However, here the gauge symmetry has been broken, and we thus need to determine what the correct conserved energy and momentum are in all local interactions, including those that violate the broken gauge charge, which we assume to take place in approximately constant background fields. By a simple calculation one can show that the "canonical" stress tensor

$$\Theta^{\mu\nu} = \bar{\psi}\gamma^{\mu} i\partial^{\nu}\psi \tag{13}$$

is, in fact, conserved in constant background fields, since from the Dirac equation derived from (1),

$$\partial_{\mu}\Theta^{\mu\nu} = (\partial^{\nu} m)\bar{\psi}\psi + g_A(\partial_{\mu}\tilde{Z}^{\nu})\bar{\psi}\gamma^{\mu}\gamma^5\psi\,. \tag{14}$$

The conserved energy and momentum are then easily calculated from the eigenstates we discussed in the preceding section and are indeed just the canonical energy $p^0 = E$ and momentum $\vec{p}$. This is as to be expected from translation invariance.

We also need to specify precisely what the fluids are, as this is ambiguous once we turn on the background in which the dispersion relations and particle eigenstates become different. In the unbroken phase we take the fluids to be the chiral eigenstates. Which states described by the dispersion relations in Fig. 1 do we take to make up the fluids described by the phase-space density in (11)? The answer is that foreshadowed by the way we wrote the dispersion relations to (4). The motivation for this choice is that most particles in these fluids are then to a good approximation in a given chiral state. This, of course, breaks down completely for low momentum states $p_z \sim m$, which are effectively equal mixtures of the chirality eigenstates. By dividing the fluids in this way, we also misdescribe the dynamics of these low momentum states by connecting the wrong branches at $p_z = 0$. Most particles in the fluid will not change direction between scattering, and so this should be a small effect. We will return to these points later. The essential point is that the effects we describe will be dominated by particles at thermal energies. The force is felt by all particles in the plasma, not just those at low momentum.

IV. FLUID EQUATIONS

We now proceed to derive in detail the truncation of the Boltzmann equations, which we have just described. The substitution of the *Ansatz* (11) in the left hand side of (10) gives, in the rest frame of the wall in which the energy is time independent,

$$-[\beta\partial_t\mu + \beta p_z\partial_t v - \partial_t\beta(E-\mu-vp_z)]f' - [\beta\partial_z\mu + \beta p_z\partial_z v - \partial_z\beta(E-\mu-vp_z)]f'\partial_{p_z}E + \beta v f'\partial_z E\,, \tag{15}$$

where $f' = (d/dx)[1/(e^x \pm 1)]$ and $x = \beta(E-\mu-vp_z)$. We take $\vec{v} = v\vec{z}$ and work to leading order in v. Making the substitution $\bar{\mu} = \mu \pm v g_A Z$ (with the sign chosen appropriately for the left-handed and right-handed particle and antiparticle fluids) and writing $p_z \pm g_A Z = k_z$, the physical momentum in the zero mass limit, we then have

$$-[\beta\partial_t\bar{\mu} + \beta k_z\partial_t v - \partial_t\beta(E-\bar{\mu}-vk_z)]f' - [\beta\partial_z\bar{\mu} + \beta k_z\partial_z v - \partial_z\beta(E-\bar{\mu}-vk_z)]f'\partial_{p_z}E + \beta v f'[\partial_z E \mp g_A\partial_z Z\cdot\partial_{p_z}E]\,. \tag{16}$$

We make this change in variables so that our equations will be in the familiar form (12) as $m \to 0$. The variable $\bar{\mu}$ is really what one would usually call the chemical potential in the $m = 0$ limit, as fluctuations in number density are proportional to it. The μ in (11) is, in fact, a gauge-dependent object, and $\bar{\mu}$ is simply the appropriate gauge-invariant chemical potential, which appears in real physical quantities calculated from the distribution function.

The crucial term here is the coefficient of the velocity v. We are working in the rest frame of the wall and so write $v = -v_w + \bar{v}$, since we are interested in the perturbations to the background, which is a plasma moving by the wall at velocity $-v_w$ in this frame. Then we see that there is a source term proportional to v_w with the coefficient

$$\beta\frac{\sqrt{p_z^2+m^2} \pm \mathrm{sgn}(p_z)g_A Z}{E}\left[\pm\mathrm{sgn}(p_z)g_A\partial_z Z\left(1 - \frac{|p_z|}{\sqrt{p_z^2+m^2}}\right) + \frac{m\partial_z m}{\sqrt{p_z^2+m^2}}\right], \tag{17}$$

where $\pm$ corresponds to the signs in the dispersion relations (4) and (5) for the particles and antiparticles in our (approximately) chiral fluids. This source manifestly vanishes as $m \to 0$ and, when integrated, will give us the force on the plasma when the wall is pushed through it. Before doing this integration of these equations, we consider also the right-hand side of the Boltzmann equation.

The collision integral $C[f]$ in (10) is equal to the rate of change of the phase-space density $f(\vec{p}, x)$ because of collisions. Considering only processes in which there are two incoming (labeled as 1 and 2) and two outgoing (labeled as $1'$ and $2'$) particles, we can write it in the form

$$\sum_{\text{processes}} \frac{1}{2(E_1 - v_w p_z)}\int_{p_{1'},p_2,p_{2'}} |\mathcal{M}|^2(2\pi)^4\delta^4(\Sigma_i p_i)\mathcal{P}[f_i]\,, \quad \mathcal{P}[f_i] = [f_1 f_2(1\mp f_{1'})(1\mp f_{2'}) - f_{1'}f_{2'}(1\mp f_1)(1\mp f_2)]\,, \tag{18}$$

where the precise spinors used as eigenstates will determine the various normalizations in the integral, $|\mathcal{M}|^2$ is the matrix element for the process, and $\mp$ is for fermions (bosons). Taking the fluid *Ansatz* (11) for each particle species and doing a perturbative expansion in $\beta = 1/T$ (about $\beta_0 = 1/T_0$), μ/T_0, and v we get, to leading order,

$$\approx \sum_{\text{processes}} \frac{1}{2(E_1 - v_w p_z)} \int_{p_{1'},p_2,p_{2'}} |\mathcal{M}|^2 (2\pi)^4 \delta^4(\Sigma_{p_i}) [f_1 f_2 (1 \mp f_{1'})(1 \mp f_{2'})]$$
$$\times \beta_0 \left[\frac{(\delta T_1 - \delta T_2)}{T_0} (E_1 - E_{1'}) + (\vec{v}_1 - \vec{v}_2) \cdot (\vec{p}_1 - \vec{p}_{1'}) + \sum (\mu_i) \right] , \tag{19}$$

where f_1, etc., are now the unperturbed distribution functions at temperature T_0. We have performed this expansion in the *plasma* frame variables for reasons we will explain below when we come to integrate this expression. The normalization factor is just the energy in the wall frame. $\sum(\mu_i)$ means a sum over chemical potentials with a positive (negative) sign for in-going (outgoing) states. In the temperature and velocity terms we have assumed that the in-going and out-going 1 and 1′ are in the same fluid and the same of 2 and 2′, since this is the case for the dominant scattering processes. For each term in brackets we must take the fastest process, which forces these fluids to the same thermal equilibrium. The ones that attenuate the temperature and velocity perturbations are gluon exchange diagrams (for quarks) or weak boson exchange (for leptons), shown in Fig. 2. These processes do not contribute to the chemical potential damping, however, since they do not change particle number. Examples of processes that do contribute are the helicity flipping gluon exchange process (as in Fig 2, but in the presence of a mass term), which can occur on the wall, and the Higgs mediated decay as that in Fig. 3, as well as sphaleron processes (both strong and weak).

We now integrate the Boltzmann equation over $\int \not{d}^3p$, $\int \not{d}^3p\, E$, and $\int \not{d}^3p\, p_z$ (*wall* frame variables) to get three moments that give us three first-order differential equations for the three functions $\delta T/T_0$, $\bar{v}$, $\bar{\mu}/T_0$ characterizing the perturbations in each fluid. In Appendix A the terms obtained by integrating the collision integral are analyzed. Considerable simplifications occur provided the integrations are done in the plasma frame variables in which f_0 has the standard (unboosted) form. Thus, we take the linear combinations $\int \not{d}^3p(E + v_w p_z)$ and $\int \not{d}^3p(p_z + v_w E)$ of the latter two integrations, which are integrations over the energy and momentum in the plasma frame (to leading order in v_w). The velocities that appear in (19) are those in the plasma frame, but the difference of velocities in this frame is equal to the difference of the velocities in the wall frame to leading order in v_w. We work perturbatively in $\delta T/T_0$, $\bar{v}$, $\bar{\mu}/T_0$ keeping the leading terms in these quantities and their derivatives, dropping next-order corrections to these coefficients in Z/T and m/T.

The equations which result are

$$\begin{aligned}
&-v_w \left(\frac{\delta T}{T_0}\right)' - a v_w \left(\frac{\bar{\mu}}{T_0}\right)' + \frac{1}{3}\bar{v}' + g v_w \left(\frac{m^2}{T_0^2}\right)' = -\bar{\Gamma}_\mu \sum \frac{\bar{\mu}}{T_0} - \Gamma_\mu \sum \left(\frac{\bar{\mu}}{T_0} \pm v_w g_A \frac{Z}{T_0}\right) , \\
&-v_w \left(\frac{\delta T}{T_0}\right)' - b v_w \left(\frac{\bar{\mu}}{T_0}\right)' + \frac{1}{3}\bar{v}' + h v_w \left(\frac{m^2}{T_0^2}\right)' = -\Gamma_T \sum \frac{\delta T}{T_0} - \bar{\Gamma}'_\mu \sum \frac{\bar{\mu}}{T_0} - \Gamma'_\mu \sum \left(\frac{\bar{\mu}}{T_0} \pm v_w g_A \frac{Z}{T_0}\right) , \\
&\left(\frac{\delta T}{T_0}\right)' + b \left(\frac{\bar{\mu}}{T_0}\right)' - v_w \bar{v}' \pm c v_w \frac{(g_A Z m^2)'}{T_0^3} = -\Gamma_v \sum \bar{v} ,
\end{aligned} \tag{20}$$

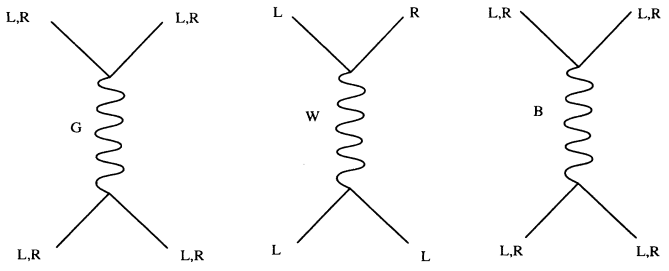

FIG. 2. Vector boson exchange diagrams that dominate in damping temperature and velocity perturbations in the fluid and play a leading role in determining the diffusion properties of different particle species. The gluon-exchange diagram also, in the presence of a quark mass term, describes the key hypercharge-violating process, namely, the helicity-flip process computed in Appendix B.

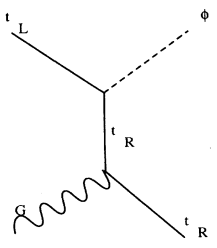

FIG. 3. Chirality flipping Higgs-boson process, which contributes to the damping of a chiral chemical potential in front of the bubble wall.

where $a = 2\zeta_2/9\zeta_3$, $b = 3\zeta_3/14\zeta_4$, $c = \ln 2/14\zeta 4$, $g = \ln 2/9\zeta_3$, $h = \zeta_2/42\zeta_4$, and ζ_n are the Riemann ζ functions ($\zeta_2 = \pi^2/6$, $\zeta_3 = 1.202$, $\zeta_4 = \pi^4/90$). To derive these equations in this form, we have expanded E, $\partial_z E$, $\partial_{p_z} E$ around $m = 0$. Except the force terms, all the terms on the left-hand side (LHS) have just the free-fluid coefficients, precisely what Eqs. (12) give if one expresses them in terms of δT, μ, v (for $m = 0$, i.e., $p = \frac{1}{3}\rho$). The positive sign in the force term applies to the L and $\bar{R}$ fluids, the negative sign to the R and $\bar{L}$ fluids; the mass is that of the appropriate fermion.

The terms on the right-hand side (RHS) require some explanation. We have written

$$\begin{aligned}
\frac{1}{3n_0}\int \not{d}^3 p C[f] &= \bar{\Gamma}_\mu \sum \frac{\bar{\mu}}{T_0} \\
&\quad + \Gamma_\mu \sum \left(\frac{\bar{\mu}}{T_0} \pm v_w g_A \frac{Z}{T_0} \right) , \\
\frac{1}{4\rho_0}\int \not{d}^3 p p_0 C[f] &= \Gamma_T \sum \frac{\delta T}{T_0} + \bar{\Gamma}'_\mu \sum \frac{\bar{\mu}}{T_0} \\
&\quad + \Gamma'_\mu \sum \left(\frac{\bar{\mu}}{T_0} \pm v_w g_A \frac{Z}{T_0} \right) , \qquad (21) \\
\frac{3}{4\rho_0}\int \not{d}^3 p p_z C[f] &= \Gamma_v \sum \bar{v} ,
\end{aligned}$$

where n_0 and ρ_0 are the unperturbed number and energy densities, respectively at T_0. To arrive at these equations, we have used symmetry arguments to show that various terms are zero for the tree-level processes we are interested in. This is discussed in Appendixes A and B.

In the collision terms as written in (19), we see that the substitution of the variable $\bar{v}$ gives the same expression with v replaced by $\bar{v}$ as it is only the relative velocity that is damped by this term. However, the substitution of $\bar{\mu} = \mu \mp v_w g_A Z \pm \bar{v} g_A Z$ is very nontrivial. The latter piece gives only a higher-order correction to our equations, but the term $v_w g_A Z$ only drops out to give the same expression with μ replaced by $\bar{\mu}$ if the charges g_A on the external legs in the process sum to zero. In the limit that the VEVs of the Higgs-boson vanish, Z is a pure gauge field for the fermions and Higgs particles, and so this cancellation occurs for all processes that conserve any linear combination of electric charge and hypercharge. Thus $\bar{\Gamma}_\mu$ and $\bar{\Gamma}'_\mu$ are calculated from decay processes that conserve hypercharge and Γ_μ and Γ'_μ from processes that explicitly violate it, the latter picking up a net contribution proportional to $v_w Z$. These latter rates, being hypercharge[1] (and T_3) violating, are VEV squared suppressed, and therefore any baryon asymmetry produced by them will vanish as the VEVs do. When the VEVs are nonzero, the Z field perturbs hypercharge-violating processes out of equilibrium locally, while the hypercharge-conserving processes remain in equilibrium, simply because they conserve the charge associated with the gauge field. These latter "see" Z as a pure gauge mode, not a real gauge-invariant field, which shifts the energies. This is precisely the type of effect that CKN called spontaneous baryogenesis. We will discuss in Sec. VI B what light this treatment throws on the question raised by Dine and Thomas in [9] about how the background should be modeled.

Before we move on to solve (20) for some specific cases, we make a few general comments.

(i) We have dropped all the time derivatives because we are interested in stationary solutions. If we wish to understand, for example, how the stationary solutions are set up at the time of nucleation, we include the terms that are obtained from the time derivatives in (16) after integration.

(ii) We have dropped all long-range fields, which result from the perturbations. This amounts to neglecting the effect of screening of electric charge and hypercharge on the solutions we will study.

These terms can easily be included (through an addition to $\vec{p}$) and give a term proportional to the field $\vec{E}$ in the third equation. Making use of Gauss' law, this can be written in terms of the perturbations, thus coupling the LHS of all the equations to one another (see Sec. VII of [6]). We will comment further on this point in the Conclusion.

(iii) As $v_w \to 0$, the only solution unperturbed at infinity is the trivial solution $\beta = \beta_0$ and $v = \mu = 0$. Any perturbation that may source a baryon number (or indeed push any process out of equilibrium) arises because of the motion of the wall. This does not mean, however, that this static equilibrium is the unperturbed one, which pertains when the field is not present. This is because the energy in the distribution function is the perturbed energy. For example, if we calculate the number density $\int \not{d}^3 p f|_{\mu=v=0}$ and subtract the true unperturbed number density, we do not get zero if we integrate, e.g., over states with $p_z > 0$. This equilibrium has in it an excess of right-moving spin-$\frac{1}{2}$ particles and an equal and opposite underdensity of left-moving spin-$(-\frac{1}{2})$ particles. The way to understand this is by analogy with an electromagnetic potential, which is screened. The thermal equilibrium reached in the presence of such a potential has an overdensity of particles in proportion to their charge. Here the "screening" of the force induced by turning on this field has the effect of dragging in particles as described by this distribution function with $v = \mu = 0$. This was the essential point made in [10], except that the energy perturbation was modeled (inappropriately) by a purely fermionic hypercharge potential.

(iv) As the VEVs of the Higgs-boson fields vanish, the only solution is again the trivial one (without time dependence), since both the mass and the rates of hypercharge-violating processes go to zero. In this case the distribution functions also describe the true unperturbed plasma, since in this limit the dispersion relation approaches the

[1]The fact that we refer to these processes as "hypercharge violating" has no particular significance. They violate any linear combination of (nonzero) hypercharge and electric charge. In particular they violate the axial charge g_A, which gives the coupling of the CP-violating condensate to the fermions and Higgs-boson fields.

pure gauge one in (4).

(v) We will explain below that in the case that we neglect the temperature fluctuations the system is reduced to the first and third equation in (20). Dropping all the force terms and setting all the decay rates to zero, to order v_w we obtain

$$b\left(\frac{\bar{\mu}}{T_0}\right)'' = -3av_w\Gamma_v\left(\frac{\bar{\mu}}{T_0}\right)', \tag{22}$$

which describes pure diffusion $\dot{n} = -D\nabla^2 n$. We can then read off the relation $D = (b/3a)\Gamma_v^{-1}$.

V. SOLUTIONS OF FLUID EQUATIONS

We now turn to the analysis of the fluid equations (20), with the goal of understanding the baryogenesis, which results from the perturbations they describe. As discussed in Sec. II of the accompanying paper [6], the anomalous baryon number violating process is perturbed from equilibrium by a difference in the distribution functions of left-handed fermions and their (right-handed) antiparticles. As we wish to study baryon production, we therefore take the difference of (20) for left-handed particles and their antiparticles, and get

$$\begin{aligned}
&-v_w\left(\frac{\delta T}{T_0}\right)' - av_w\left(\frac{\bar{\mu}}{T_0}\right)' + \frac{1}{3}\bar{v}' = -\bar{\Gamma}_\mu\sum\left(\frac{\bar{\mu}}{T_0}\right) - \Gamma_\mu\sum\left(v_w g_A\frac{Z}{T_0}\right),\\
&-v_w\left(\frac{\delta T}{T_0}\right)' - bv_w\left(\frac{\bar{\mu}}{T_0}\right)' + \frac{1}{3}\bar{v}' = -\Gamma_T\left(\frac{\delta T}{T_0}\right) - \bar{\Gamma}'_\mu\sum\left(\frac{\bar{\mu}}{T_0}\right) - \Gamma'_\mu\sum\left(v_w g_A\frac{Z}{T_0}\right),\\
&\left(\frac{\delta T}{T_0}\right)' + b\left(\frac{\bar{\mu}}{T_0}\right)' - v_w\bar{v}' + F(z) = -\Gamma_v\bar{v}\,.
\end{aligned} \tag{23}$$

We have compactified our notation: $\bar{\Gamma}_\mu$ now includes *all* decay processes, and Γ_μ denotes only the hypercharge violating ones. The force terms in the first two equations in (20) cancel out because the gradient in the real mass affects particles and antiparticles equally. The parameters $\delta T, \bar{v}, \bar{\mu}$ now represent the *difference* in these quantities for particles and antiparticles, and the force

$$F = 2cv_w g_A\frac{(Zm^2)'}{T_0^3} \equiv Av_w\frac{(Zm^2)'}{T_0^3}\,. \tag{24}$$

We have used the fact that particles and antiparticles couple in exactly the same way in the gauge boson exchange diagrams to cancel out the temperature and velocity perturbations of the other fluids. This removes the sum in the Γ_T and Γ_v terms. The counting factor that results, over particles and antiparticles of all flavors, has been absorbed in the definition of Γ_T and Γ_v. For quarks we show in Appendix A that

$$\Gamma_v = 3\Gamma_T \simeq \alpha_s^2\ln\frac{1}{\alpha_s}T \simeq \frac{T}{20}\,. \tag{25}$$

We note that the relation $D = b/(3a\Gamma_v)$ from (22) then gives $D \simeq 5/T$, in very good agreement with the value calculated by a different method in [6]. The only coupling to perturbations in other fluids remains in the sums for the decay processes. There are two distinct sources in (23) for the perturbations: the force terms $F(z)$; the hypercharge-violating processes, which are perturbed from equilibrium as the wall passes when $v_w Z \neq 0$. As the equations are linear we can separate these sources and study them independently.

We will not attempt to solve the full set of equations in complete generality for each of these two source terms. First, we will limit our scope by considering only the case where the source terms directly affect the *top quark*. Both the classical force term and (we will see below) the spontaneous baryogenesis terms are proportional to the mass squared of the fermion for which (23) describe the particle minus antiparticle perturbations. We will thus work in the approximation that only the top quark Yukawa coupling is nonzero, which is good if the fermion Yukawa couplings are (as in the minimal standard model) proportional to their zero-temperature masses. We will not consider the case emphasized in [6], where in a two-Higgs-boson extension the τ lepton can have a Yukawa coupling as large as that of the top quark (and hence a comparable finite-temperature tree-level mass).

We now discuss (i) dropping the temperature fluctuations, and thus reducing the equations to just two coupled equations for $\bar{\mu}$ and $\bar{v}$, which can in turn be written as two second-order uncoupled equations for these two variables, (ii) the solution of the reduced equations for the classical force source term with the simplification that we neglect all decay processes, (iii) the problem with decay processes included, for the classical force source term, and (iv) the source terms from hypercharge-violating processes and how they source baryogenesis.

A. Thermalization and validity of the fluid *Ansatz*

In Sec. III we explained that we do not expect the temperature fluctuations to accurately reflect the perturbations in the plasma because the tree-level gauge boson exchange processes, which damp them away, are exactly the same processes that damp away the perturbations to the distribution functions, which we neglected in taking the *Ansatz* (11). We kept them in our *Ansatz*, however, in order to have a quantitative measure of the validity of our approximation. It is this point that we first consider here.

Neglecting all decay processes, Eqs. (23) are

$$-v_w\frac{\delta T'}{T_0} - av_w\frac{\bar{\mu}'}{T_0} + \frac{1}{3}\bar{v}' = 0\,,$$

$$-v_w\frac{\delta T'}{T_0}-bv_w\frac{\bar{\mu}'}{T_0}+\frac{1}{3}\bar{v}'=-\Gamma_T\frac{\delta T}{T_0}\,,\qquad(26)$$
$$\frac{\delta T'}{T_0}+b\frac{\bar{\mu}'}{T_0}-v_w\bar{v}'+F(z)=-\Gamma_v\bar{v}\,.$$

One can convert these to a pair of second-order uncoupled equations for δT and $\bar{\mu}$ (by integrating the first equation directly to find $\bar{v}$), and then solve them for various sources F. We will not present here the details of this calculation, as the results are of no importance except for the following point. Two parameters, $\lambda_D L$ and $\lambda_T L$, enter in determining the behavior of the solutions, where

$$\lambda_D=\frac{v_w}{D},\quad \lambda_T=\frac{b}{b-a}\frac{\Gamma_T}{v_w}\qquad(27)$$

are the two roots of (26) and L is the thickness of the wall. The diffusion root λ_D describes the diffusion tail in front of the wall, while λ_T describes the decay of perturbations behind the source. $\lambda_D L$ is simply the squared ratio of the wall thickness to the distance a particle with diffusion constant D diffuses as the wall passes ($\sim\sqrt{Dt}\sim\sqrt{DL/v_w}$); this is the parameter that, as we discuss below, will characterize what we call "good transport" or "poor transport." $\lambda_T L$ is the ratio of the time of passage of the wall (L/v_w) to the mean free time for temperature attenuating processes ($\sim\Gamma_T^{-1}$), and it is a measure of how efficiently the temperature perturbations are damped on the wall. One finds that when $\lambda_T L>1$, the temperature perturbations in the solutions to (26) are damped by at least $1/\lambda_T L$ relative to the chemical potential fluctuations. Examining (26), one can, in fact, see this damping directly in the second equation. Taking all the derivatives to go as L^{-1}, we see immediately that the suppression follows. When one incorporates the decay processes a similar conclusion follows provided $\Gamma_T\gg\Gamma_\mu$, which applies (see rates given below).

Because this condition for the damping of temperature fluctuations is the same as that of the validity of our initial *Ansatz*, we always take it to apply and reduce our equations to the first and third in (23) with δT set equal to zero. Noting the relation between Γ_T and Γ_v from (25) and $\Gamma_v=b/3aD^{-1}$ from (22), the condition becomes

$$v_w<\frac{L}{3D}\quad\text{thermalization}\,.\qquad(28)$$

Still neglecting the decay processes, the equations simplify further:

$$-av_w\frac{\bar{\mu}'}{T_0}+\frac{1}{3}\bar{v}'=0\,,$$
$$b\frac{\bar{\mu}'}{T_0}-v_w\bar{v}'+Av_w\frac{(Zm^2)'}{T_0^3}=-\Gamma_v\bar{v}\,,\qquad(29)$$

where $A=2cg_A$. The solution to the first equation gives $\bar{v}=3av_w(\bar{\mu}/T_0)$ (using the boundary condition that $\bar{\mu}=\bar{v}=0$ far in front of the wall) and substituting in the second equation, again using the relation $\Gamma_v=(b/3a)D^{-1}$ from (22), we get (to leading order in v_w)

$$D\frac{\bar{\mu}'}{T_0}+v_w\frac{\bar{\mu}}{T_0}=-\frac{D}{b}F(z)\,.\qquad(30)$$

As discussed in Sec. III, $\bar{v}$ is, like δT, not in itself to be taken to accurately describe the perturbations in the fluid. This is the case because we would expect there to be other anisotropic (in momentum) components of a general distribution function, which we have neglected in our *Ansatz*, which will be damped away by the same (tree-level gluon exchange) processes at approximately the same rate as the perturbation parametrized by $\bar{v}$, which we have taken. We cannot, however, consistently set it to zero in (23); but, as we now see, $\bar{v}$ is indeed damped by v_w relative to $\bar{\mu}$, so that it will not itself contribute (at leading order in v_w) to the biasing of the baryon number violating processes, and neither does it enter in (30), which determines $\bar{\mu}$. Its only role is to mediate the force to the chemical potential, and we assume that any other anisotropic component would have led to approximately the same result.

The fluid equations (26) are calculated to leading order in v_w. A fuller analysis incorporating all orders in v_w can be performed and shows that the velocity at which the leading-order analysis breaks down is the speed of sound $v_w\sim v_s=1/\sqrt{3}$ in the plasma. If the wall moves faster than this, there is no solution in front of the wall, and perturbations cannot propagate into this region. We are interested in the case when perturbations can propagate in front of the wall where the anomalous electroweak processes are unsuppressed. Thus, we assume

$$v_w<v_s=\frac{1}{\sqrt{3}}\,.\qquad(31)$$

B. Classical force sourced perturbations without decay

We now solve (30) for a chosen *Ansatz* for the force term in order to illustrate the behavior of the perturbations they describe and to gain some simple intuition for the more complex case where we include the decay terms. We take the following "ramp" *Ansatz* for the source term:

$$Av_w\frac{Zm^2}{T_0^3}=\begin{cases}F_0\left(z-\dfrac{L}{2}\right), & -\dfrac{L}{2}<z<\dfrac{L}{2},\\ 0, & \text{otherwise},\end{cases}\qquad(32)$$

where F_0 is the constant force on the wall, and, as above, $A=2cg_A$. Equation (30) then has a particular solution, which is nonzero only on the wall, and a homogeneous solution, which is an exponential describing pure diffusion $\sim\exp[-(v_w/D)z]$. We impose the boundary conditions

$$D\left(\frac{\bar{\mu}}{T_0}\right)\Bigg|_{L/2-\epsilon}^{L/2+\epsilon}=0,\quad D\left(\frac{\bar{\mu}}{T_0}\right)\Bigg|_{-L/2-\epsilon}^{-L/2+\epsilon}=\frac{DLF_0}{b}\qquad(33)$$

obtained by integrating (30) taking $\bar{\mu}$ to be at most step discontinuous across the boundaries (so that its integral is continuous). Solving, requiring $\bar{\mu}$ to be finite at $-\infty$, we get

$$\frac{\mu}{T_0} = \frac{F_0 L}{b} \begin{cases} 0, & z < -\frac{L}{2}, \\ -\frac{D}{v_w L} + \left(\frac{D}{v_w L} + 1\right) \exp\left[-\frac{v_w}{D}\left(z + \frac{L}{2}\right)\right], & -\frac{L}{2} < z < \frac{L}{2}, \\ \left\{\exp\left(-\frac{v_w}{D}L\right) - \frac{D}{v_w L}\left[1 - \exp\left(-\frac{v_w}{D}L\right)\right]\right\} \exp\left[-\frac{v_w}{D}\left(z - \frac{L}{2}\right)\right], & z > \frac{L}{2}. \end{cases} \tag{34}$$

These solutions for $\bar{\mu}/T_0$ are sketched in Fig. 4 for the two cases (i) $v_w L/D \ll 1$ and (ii) $v_w L/D \gg 1$, when the solutions on the wall can be written

$$\frac{-F_0 L}{b} \begin{cases} \frac{1}{2}\frac{v_w L}{D} + \frac{\left(z - \frac{L}{2}\right)}{L}\left[1 - \frac{1}{2}\left(\frac{v_w L}{D}\right)2\right], & \frac{v_w L}{D} \ll 1, \\ \frac{D}{v_w L}, & \frac{v_w L}{D} \gg 1. \end{cases} \tag{35}$$

In the first case we see that the solution mimics the behavior of the driving force. From (29) one can see that this behavior is generic for $v_w L/D \ll 1$, for expanding in v_w one finds at leading order the solution

$$\bar{v} = 0, \quad \frac{\bar{\mu}}{T_0} = -v_w \frac{A}{b}\frac{Zm^2}{T_0^3} \tag{36}$$

is nonzero only on the wall. What the parameter $v_w L/D$ tells us is how efficient the diffusion is in bringing us to (36). As discussed in Sec. V A it is simply a ratio of the thickness of the wall to the distance a particle diffuses as the wall passes. This is the parameter that defines good transport. The corrections to (36) describe a diffusion tail in front of the wall which has amplitude

$$\left.\frac{\bar{\mu}}{T_0}\right|_{L/2} = -\frac{1}{2}\frac{v_w L}{D}\frac{F_0 L}{b}. \tag{37}$$

The factor of 2 arises from the fact that the diffusion in front of the wall is driven by the average amplitude of the potential on the wall, since particles are in this regime "seeing" the whole wall. This is confirmed (see examples later) by calculating with other *Ansätze*. We thus conclude that, more in general, we would find the solution in front of the wall,

$$\frac{\bar{\mu}}{T_0} = +\frac{v_w L}{D} v_w \frac{A}{b}\frac{\langle Zm^2\rangle}{T_0^3} \exp\left[-\frac{v_w}{D}\left(z - \frac{L}{2}\right)\right], \tag{38}$$

where angular brackets denote the average value on the wall.

When $v_w L/D \gg 1$, i.e., when the transport is "poor" over the relevant timescales, the solution looks like that in Fig. 4(b). The amplitude on the wall rapidly approaches that in front of the wall, which is

$$\left.\frac{\bar{\mu}}{T_0}\right|_{L/2} = -\frac{D}{v_w L}\frac{F_0}{b}, \tag{39}$$

so that the integrated amplitude $\int_{L/2}^{\infty} \bar{\mu}$ is suppressed relative to the good transport case by $(D/v_w L)^2$. It is this integrated amplitude of $\bar{\mu}$ (recall that it is the *difference* of particle and antiparticle chemical potentials) in front of the wall that will be the effective driving force for the final baryon asymmetry, when we assume the baryon number violating processes are immediately switched off on the wall. We note that the solutions (34) have the property that

$$\int_{-\infty}^{+\infty} \bar{\mu}(z) dz = 0. \tag{40}$$

In fact, this can be shown directly by integrating (30) once and taking the solutions to be zero at $\pm\infty$. The integral of the chemical potential is zero because there is no net particle minus antiparticle creation in the absence of the decay processes. Thus, the integrated contribution in front of the wall exactly cancels that on the wall, the excess of particles pulled onto the wall in response to the force being exactly cancelled by a deficit in the diffusion tail in front of the wall. In terms of baryon production, it follows that, if the sphaleron rate were unsuppressed on the wall, exact cancellation would occur between the production in front of and on the wall so the source would not bias net baryon production. The extent of the cancellation that can occur is a sensitive function of the wall profile, but, unless Z condenses, only where the VEV is very small this will not be significant. We will always assume that the baryon number violating processes are only turned on in front of the wall.

This property (40) allows us to read off simply from (36) the integrated amplitude in front of the wall when $v_w L/D \ll 1$ (to leading order in this parameter) as

FIG. 4. Solutions for the chiral chemical potential μ in the background of a bubble wall, with a ramp *Ansatz* for the CP-violating condensate field $m^2 Z$ (solid lines). The solutions for $\bar{\mu}/T_0$ are sketched (dashed lines) for the two cases (i) $v_w L/D \ll 1$ and (ii) $v_w L/D \gg 1$.

$$\int_{L/2}^{\infty} \frac{\bar{\mu}}{T_0} = v_w \frac{A}{b} \int_{\text{wall}} \frac{Zm^2}{T_0^3}\,, \tag{41}$$

where again $A = 2cg_A$ [c and b being the numbers defined after (20)]. This, in fact, also proves (38), since we know that the solution in front of the wall $\sim e^{-(v_w/D)z}$. We note that the result is in this regime independent of D and L, and we will see that the factor of v_w also drops out when we calculate the baryon asymmetry. We will defer doing so explicitly until after the next section, in which we discuss incorporating the decay processes in this analysis.

C. Decay processes and baryon production

Putting back the decay rates our equations are

$$-av_w \left(\frac{\bar{\mu}}{T_0}\right)' + \frac{1}{3}\bar{v}' = -\bar{\Gamma}_\mu \sum \frac{\bar{\mu}}{T_0} + \Gamma_\mu \sum v_w g_A \frac{Z}{T_0}\,, \tag{42}$$

$$b\left(\frac{\bar{\mu}}{T_0}\right)' + F(z) = -\Gamma_v \bar{v}\,,$$

where we follow again the conventions in (23). $\bar{\mu}$ is again the *difference* in particle and antiparticle chemical potentials, and the sums are over the external legs of the processes, which change the number of particles minus antiparticles. We have a pair of such equations for each fermion of (approximate) chirality, where $F = \pm A v_w [(Zm^2)'/T_0^3]$ (+ for the $L - \bar{L}$ perturbations and − for the $R - \bar{R}$ perturbations) and m is the mass of the fermion, which we have assumed only to be nonzero for the top quark. The equations are coupled only through the sums in the decay terms on the right-hand side, and it is this coupling that we now consider.

As before, we can decouple the variables $\bar{\mu}$ and $\bar{v}$ and concentrate on a set of second order equations for the $\bar{\mu}$:

$$D\frac{\bar{\mu}''}{T_0} + v_w \frac{\bar{\mu}'}{T_0} - \bar{\Gamma}_\mu \sum \frac{\bar{\mu}}{T_0} = -\frac{D}{b} F'(z) - \Gamma_\mu \sum v_w g_A \frac{Z}{T_0}\,. \tag{43}$$

The decay rates here have absorbed a factor of $1/a$ relative to the rates defined in (21). There are a similar set of equations for the $\bar{v}$. We will not consider these further, since, as discussed in Sec. V A, $\bar{v}$ is attenuated relative to $\bar{\mu}$ and hence also its effect on the baryon number violating processes, which is what concerns us here.

What are the decay processes? Recall that our particle and antiparticle states are those of our (approximately) chiral fluids. They are the WKB eigenstates of the dispersion relations (4) and (5), which become pure chirality states in the unbroken phase.

In the broken phase they are helicity states, which are mixtures of the two chiralities.

It is thus natural that we divide the processes into (i) those that occur in both phases and (ii) those that occur only in the broken phase. We consider these in turn.

(i) In the unbroken phase our states are exact chirality eigenstates. The only perturbative processes that change chirality are those involving Higgs particles, such as that shown in Fig. 3, in which a left-handed quark flips chirality when it scatters off a gluon and emits a Higgs particle. Since we are taking only the Higgs-boson–top Yukawa coupling to be nonzero, this induces a coupling only between left-handed top quarks, right-handed top quarks, and Higgs particles. The gluon cancels out when we subtract particles from antiparticles because it is its own antiparticle. The only other processes changing the number of particles of a given chirality in the unbroken phase are the strong anomalous processes, and the weak anomalous processes, which are responsible for the baryon production. The former couple left-handed quarks of all flavors to right-handed quarks of all flavors directly; the latter couple all the left-handed quarks to all the left-handed leptons.

(ii) In the broken phase all the processes in the unbroken phase (except the baryon number violating processes) are still present, but there are many additional processes that couple particles on a given branch of our dispersion relations to other particle states because of the mixing of helicity and chirality states when the mass is nonzero.

When we calculate interactions between particles in these states, we find that they can couple to one another through a "helicity-flipping" gauge boson exchange. This is also an example of what we called a "hypercharge-violating" process: If we identify the in-going states by the hypercharge of the state they deform into in the unbroken phase, and hypercharge is not conserved. We have evaluated the rate for this process in Appendix B. There are many other such processes, e.g., involving Higgs-boson fields. There are also many flavor changing processes mediated by W bosons, but these are zero in the approximation that only the top-quark Yukawa coupling is nonzero.

We now make three further simplifications. First we will assume that the baryon number violating processes can be neglected, except in their role as the source of the net baryon number. We will see below that the condition that this be true is (see also [6])

$$\Gamma_s < \frac{v_w^2}{D} \tag{44}$$

where Γ_s is the rate for electroweak anomalous processes. v_w^2/D is just the rate of capture of a diffusing particle by the advancing wall (the inverse of the time it spends diffusing before capture).

The second further simplification we make is to neglect completely the decay processes in the unbroken phase involving Higgs particles on the external legs. The reason we do this is found in the study of these processes in [6]—in the unbroken phase Eqs. (43) are precisely the same diffusion-decay equations obtained there. The change to the results when these decay processes were incorporated was found to be a minor numerical one, and we assume that the same will be true here. In short, the reason is that these processes do not drive the quantity sourc-

ing baryon number (i.e., left-handed fermion perturbations) to zero. In the limit where they are fast enough to equilibrate locally they simply lead to a redistribution of particles amongst the left-handed fermions, right-handed fermions, and Higgs particles.

The final simplifying assumption we make is to take the diffusion constant of left-handed and right-handed quarks to be equal. Although this is a very good approximation, since the diffusion properties are dominated by the strong interactions, it is one that must be treated with caution in certain limits of extreme suppression of baryon production by the decay processes. This is discussed in Sec. VI of [6], and the treatment given there can be applied to the present case. We will not discuss this here.

With these assumptions, we can now greatly simplify the full set of coupled equations (43) for all species in the plasma. Defining the variables

$$\bar{\mu}_t = N_c(\bar{\mu}_{t_L} - \bar{\mu}_{t_R}),\ \ \bar{\mu}_\Delta = N_c\Sigma_i(\bar{\mu}^i_{qL} - \bar{\mu}^i_{qR}),$$
$$\bar{\mu}_B = N_c\Sigma_i(\bar{\mu}^i_{qL} + \bar{\mu}^i_{qR}), \tag{45}$$

where $\bar{\mu}_{t_L}$ means the difference in the chemical potential of the left-handed top and its (right-handed) antiparticle, etc., the sum is over flavors, and N_c is the number of colors, we can extract a simple set of three coupled equations:

$$D\frac{\bar{\mu}_t''}{T_0} + v_w\frac{\bar{\mu}_t'}{T_0} - \Gamma_f\frac{\bar{\mu}_t}{T_0} - \frac{\Gamma_{ss}}{N_f}\frac{\bar{\mu}_\Delta}{T_0} = -\frac{D}{b}F'(z) - 2N_c\Gamma_f v_w g_A\frac{Z}{T_0},$$
$$D\frac{\bar{\mu}_\Delta''}{T_0} + v_w\frac{\bar{\mu}_\Delta'}{T_0} - \Gamma_f\frac{\bar{\mu}_t}{T_0} - \Gamma_{ss}\frac{\bar{\mu}_\Delta}{T_0} = -\frac{D}{b}F'(z) - 2N_c\Gamma_f v_w g_A\frac{Z}{T_0},$$
$$D\frac{\bar{\mu}_B''}{T_0} + v_w\frac{\bar{\mu}_B'}{T_0} - \Gamma_s\frac{\bar{\mu}_B}{T_0} = +\Gamma_s\frac{\bar{\mu}_\Delta}{T_0}, \tag{46}$$

where $F = 4cN_c v_w g_A[(Zm^2)'/T_0^3]$. N_f is the number of fermion flavors, and we see that the first two equations reduce to a single one in the case $N_f = 1$. Γ_f, Γ_{ss}, and Γ_s are the rates for the helicity flipping, strong anomalous processes and weak anomalous processes respectively. With this new convention, Eqs. (46) take the form of diffusion equations corresponding to those in the companion paper [6], and the rates Γ are identical to the rates used there. Γ_{ss} and Γ_s can be read off from [6], and the helicity flip rate is derived in Appendix B:

$$\Gamma_f \approx \frac{1}{2}\frac{m_t^2}{T^2}\alpha_s^2 T \approx \frac{1}{100}\frac{m_t^2}{T},$$
$$\Gamma_{ss} = \frac{32N_f}{3}\kappa_{ss}\alpha_s^4 T \approx \kappa_{ss}\frac{T}{40}, \tag{47}$$
$$\Gamma_s = 9N_F\kappa_s\alpha_w^4 T \approx \kappa_s\frac{T}{3\times 10^4},$$

where $\frac{8}{3}\kappa_{ss}\alpha_s^4 T^4$ and $\kappa_s\alpha_s^4 T^4$ are the number of strong and weak (respectively) anomalous processes per unit volume per unit time N_F is the number of fermion families.

Before proceeding to analyze these equations and calculate the baryon asymmetry, we stop and review the numerous assumptions we have made in deriving the equations (46).

Assumption 1. $L > 1/T$, so that most particles in the plasma are indeed accurately described by the WKB approximation. Typical wall thicknesses are $L \sim 20/T$.

Assumption 2. $v_w < L/3D$, the "thermalization" condition for the applicability of our fluid *Ansatz*. We calculated $D \approx 5/T$, so for a typical thick wall $L \sim 20/T$ this is extremely good for any wall velocity.

Assumption 3. $v_w < 1/\sqrt{3}$. We work to linear order in the wall velocity assumed smaller than the speed of sound in the plasma, so that perturbations can propagate into the region in front of the wall and give "nonlocal" baryogenesis. This restricts us to modest wall velocities.

Assumption 4. $\Gamma_s < v_w^2/D$, so that the back reaction of the baryon number violating processes on the perturbed quantities can be neglected. Using (25) we see that this corresponds to $v_w > 10^{-2}\sqrt{\kappa_s}$. Numerical simulations indicate $\kappa_s \sim 0.1 - 1$ so this is consistent with favored wall velocities $v_w \sim 0.1 - 1$. If $\Gamma_s > v_w^2/D$, the sphaleron rate can equilibrate in front of the wall.

Assumption 5. All decay processes involving Higgs particles on the external legs can be neglected. This can be revised along the lines discussed in [6] and should lead only to minor numerical corrections.

Assumption 6. The diffusion constants of quarks of opposite chirality can be taken to be equal. A very good approximation, this needs only to be revised for the limit of extreme suppression of an asymmetry by decay processes.

Assumption 7. Only the top-quark Yukawa coupling is nonzero, so we do not describe the case of a two doublet model in which the lepton Yukawa coupling may be large.

VI. THE BARYON ASYMMETRY

The baryon number density $B = (1/N_c)(T^2/12)\bar{\mu}_B$, and, calculating with the last equation in (46), we find its value at the front of the wall to be

$$B_0 = \frac{1}{N_c}\frac{T^2}{12}\bar{\mu}_B \approx \frac{1}{N_c}\frac{T^2}{12}\frac{\Gamma_s}{v_w}\int_{L/2}^{\infty}\bar{\mu}_\Delta(z)dz. \tag{48}$$

This is the final value of the baryon number in the broken phase under the assumption that the baryon number violating processes are turned off everywhere in the broken phase. The expression (48) is valid with the assumption we made that Γ_s satisfies $v_w^2/\Gamma_s D \gg 1$.

To determine the final baryon asymmetry we must use the first two equations in (46) to extract $\bar{\mu}_\Delta$ in front of the wall, which is the effective source for the baryon production. We will not solve exhaustively the two coupled equations for $\bar{\mu}_t$ and $\bar{\mu}_\Delta$ in (46) but will limit ourselves to the case that the dominant decay process is Γ_{ss} so that we can drop the term $\Gamma_f\bar{\mu}_t$ in the second equation

in (46). This is justified for all κ_{ss} in the range 0.1–1, since $m_t^2 < T^2/4$ on the wall [cf. (47)]. We are then left with a single equation for $\bar{\mu}_\Delta$:

$$D\frac{\bar{\mu}_\Delta''}{T_0} + v_w\frac{\bar{\mu}_\Delta'}{T_0} - \bar{\Gamma}_\mu\frac{\bar{\mu}_\Delta}{T_0} = -\frac{D}{b}F'(z) - 2N_c\Gamma_\mu v_w g_A\frac{Z}{T_0}\,. \tag{49}$$

To solve (49) we need to find particular solutions as well as solutions to the homogeneous equation. The latter are $\sim e^{-\lambda z}$, where

$$\lambda = \left\{ \begin{array}{l} \lambda_D = \dfrac{v_w}{D}\left(1 + \dfrac{D\bar{\Gamma}_\mu}{v_w^2} + \cdots\right) \text{ and } -\lambda_d = -\dfrac{\bar{\Gamma}_\mu}{v_w}\left(1 - \dfrac{D\bar{\Gamma}}{v_w^2} + \cdots\right), \quad \dfrac{D\bar{\Gamma}_\mu}{v_w^2} \ll 1, \\ \pm\lambda_\pm = \pm\left[\left(\sqrt{\dfrac{\bar{\Gamma}_\mu}{D}} + \cdots\right) \mp \dfrac{v_w}{2D}\right], \quad \dfrac{D\bar{\Gamma}_\mu}{v_w^2} \gg 1. \end{array} \right\} \tag{50}$$

The behavior of the solutions is determined by the parameter $D\bar{\Gamma}_\mu/v_w^2$ (precisely as in the companion appear [6]). It characterizes the competition between decay and diffusion, D/v_w^2 being the time a typical particle spends diffusing in front of the wall before being caught. When $D\bar{\Gamma}_\mu/v_w^2 \ll 1$, decay becomes irrelevant in front of the wall, and the only effect of the decay processes is to restore thermal equilibrium far behind the wall. This is also the criterion we need to use to see if any process is of relevance to the problem we are considering. In particular, we used it above in (44) and implicitly in assuming that the Yukawa couplings, which we have set to zero, mediate decay processes that are slow in precisely this sense. We now consider the solution of (49) for each of the two source terms on the right-hand side separately.

A. Classical force baryogenesis

We return again to the "ramp" *Ansatz* (32), with $A = 4cN_c$, and take only the force term as a source in (49). The problem is now homogeneous with boundary conditions

$$\begin{aligned} D\left(\frac{\bar{\mu}_\Delta}{T_0}\right)' + v_w\left(\frac{\bar{\mu}_\Delta}{T_0}\right)\Bigg|_{\pm L/2-\epsilon}^{\pm L/2+\epsilon} &= \pm\frac{DF_0}{b}\,, \\ D\left(\frac{\bar{\mu}_\Delta}{T_0}\right)\Bigg|_{L/2-\epsilon}^{L/2+\epsilon} &= 0\,, \\ D\left(\frac{\bar{\mu}_\Delta}{T_0}\right)\Bigg|_{-L/2-\epsilon}^{-L/2+\epsilon} &= \frac{DLF_0}{b}\,, \end{aligned} \tag{51}$$

derived by integrating (49) with the assumption that the integral of $\bar{\mu}_\Delta$ is continuous across the boundaries. Requiring $\bar{\mu}_\Delta$ to be finite at $\pm\infty$, we take

$$\bar{\mu}_\Delta = \left\{ \begin{array}{ll} A_f e^{-\lambda_f z}, & z > \dfrac{L}{2}, \\ A_w e^{-\lambda_f z} + B_w e^{\lambda_b z}, & -\dfrac{L}{2} < z < \dfrac{L}{2}, \\ B_b e^{\lambda_b z}, & z < -\dfrac{L}{2}, \end{array} \right. \tag{52}$$

where A_f, A_w, B_w, and B_b are constants, and from (50) we have

$$\lambda_f = \left\{ \begin{array}{ll} \lambda_D & \dfrac{D\bar{\Gamma}_\mu}{v_w^2} \ll 1, \\ \lambda_+ & \dfrac{D\bar{\Gamma}_\mu}{v_w^2} \gg 1, \end{array} \right. \qquad \lambda_b = \left\{ \begin{array}{ll} \lambda_d & \dfrac{D\bar{\Gamma}_\mu}{v_w^2} \ll 1, \\ \lambda_- & \dfrac{D\bar{\Gamma}_\mu}{v_w^2} \gg 1. \end{array} \right. \tag{53}$$

Using the boundary conditions, we determine the solution in front of the wall to be

$$-\frac{1}{b}F_0\left(\frac{1}{(\lambda_f+\lambda_b)L} - \frac{(\lambda_b+\lambda_D^0)L}{(\lambda_b+\lambda_f)L}e^{-\lambda_f L}\right)e^{-\lambda_f(z-L/2)}\,, \tag{54}$$

where $\lambda_D^0 = v_w/D$. In various limits this reduces to

$$v_w\frac{A}{b}\frac{Z_0 m_0^2}{2T_0^3}\left\{ \begin{array}{l} \dfrac{v_w L}{D}\exp\left[-\dfrac{v_w}{D}\left(z-\dfrac{L}{2}\right)\right], \quad \dfrac{v_w L}{D} \ll 1 \text{ and } \dfrac{D\bar{\Gamma}_\mu}{v_w^2} \ll 1, \\ \dfrac{2D}{v_w L}\exp\left[-\dfrac{v_w}{D}\left(z-\dfrac{L}{2}\right)\right], \quad \dfrac{v_w L}{D} \gg 1 \text{ and } \dfrac{D\bar{\Gamma}_\mu}{v_w^2} \ll 1, \\ \dfrac{1}{2}\sqrt{\dfrac{\bar{\Gamma}_\mu}{D}}L\exp\left[-\sqrt{\dfrac{\bar{\Gamma}_\mu}{D}}\left(z-\dfrac{L}{2}\right)\right], \quad \sqrt{\dfrac{\bar{\Gamma}_\mu}{D}}L \ll 1 \text{ and } \dfrac{D\bar{\Gamma}_\mu}{v_w^2} \gg 1, \\ \dfrac{1}{L}\sqrt{\dfrac{D}{\bar{\Gamma}_\mu}}\exp\left[-\sqrt{\dfrac{\bar{\Gamma}_\mu}{D}}\left(z-\dfrac{L}{2}\right)\right], \quad \sqrt{\dfrac{\bar{\Gamma}_\mu}{D}}L \gg 1 \text{ and } \dfrac{D\bar{\Gamma}_\mu}{v_w^2} \gg 1, \end{array} \right. \tag{55}$$

where $Z_0 = Z(-L/2)$ and $m_0 = m(-L/2)$.

The first two cases agree precisely with what we saw when we analyzed the force neglecting decay processes in Sec. V B. The prefactor in (55) corresponds to the average of the solution approached on the wall for $v_w L/D \ll 1$, but with the opposite sign so that the integrated contribution in front of the wall cancels that on the wall. The two limits for $v_w L/D$ are the limits of good and poor transport, which we discussed.

The two other cases given in (55) tell us how these solutions are modified when $D\bar{\Gamma}_\mu/v_w^2 > 1$. The penetration of the diffusion solutions into the unbroken phase is reduced, since $\sqrt{\bar{\Gamma}_\mu/D} > v_w/D$. As we noted, this is just the condition that the average diffusing particle's time in the unbroken phase before capture be longer than its decay lifetime. A second parameter enters in determining how the amplitude of the solution in front of the wall is changed. In the first case, $\sqrt{\bar{\Gamma}_\mu/D}L \ll 1$, the amplitude, in fact, compensates by increasing so that the integrated result $\int_{L/2}^{\infty} \bar{\mu}_\Delta$ is unchanged (up to a factor of 2). In the second case, $\sqrt{\bar{\Gamma}_\mu/D}L \gg 1$, the amplitude is attenuated, and the integrated result differs from that in the no-decay case by a factor of $v_w^2/2D\bar{\Gamma}_\mu \ll 1$. The physical meaning of the parameter $\sqrt{\bar{\Gamma}_\mu/D}L$ is also simple. It is (the square root of) the ratio of the time a particle takes to diffuse across the wall to its decay lifetime. So what the third and fourth cases in (55) tell us is that the net density of particles in front of the wall in these stationary solutions is not changed (up to a factor of 2) unless the decay process is fast enough so that particles can decay as they cross the wall. This is a surprising result, as one might expect the only relevant parameter to be $D\bar{\Gamma}_\mu/v_w^2$, which compares the decay time to the time a particle actually spends in front of the wall.

The factor of 2 has a simple explanation, which will be familiar to the close reader of [6]. If one considers a diffusion/decay equation for a single species with a given injected flux modeled by a δ function, one finds two distinct regimes corresponding to the value of $\Gamma D/v_w^2$. In the high-velocity diffusion regime ($\Gamma D/v_w^2 \ll 1$) the stationary solution puts most of the injected flux into the amplitude in front of the wall; in the low-velocity case the solution has equal and opposite amplitude in front and behind, sharing the injected flux so that the amplitude is exactly half that in the first case.

One might worry that some of these features are artifacts of our *Ansatz* (32) in which there is a discontinuity in the profile of $m^2 Z$ at the back of the wall. To check this, we take instead the "bell" *Ansatz*:

$$Av_w \frac{Zm^2}{T_0^3} = \begin{cases} \dfrac{F_0 L}{4}\left(1 - \dfrac{4z^2}{L^2}\right), & -\dfrac{L}{2} < z < \dfrac{L}{2}, \\ 0, \text{ otherwise}, \end{cases} \tag{56}$$

and using the same conventions as in (52), we find in front of the wall

$$-\frac{1}{b}F_0 \frac{1}{(\lambda_f + \lambda_b)}\left(\frac{2\lambda_b}{\lambda_d^0}\frac{1}{\lambda_D^0 L}(1 - e^{-\lambda_f L}) - (1 + e^{-\lambda_f L})\right) e^{-\lambda_f (z - L/2)}, \tag{57}$$

where $\lambda_d^0 = \bar{\Gamma}_\mu/v_w$ and $\lambda_D^0 = v_w/D$. In the same limits as before this reduces to

$$\frac{F_0}{6b}\begin{cases} \dfrac{v_w L}{D}\exp\left[-\dfrac{v_w}{D}\left(z - \dfrac{L}{2}\right)\right], & \dfrac{v_w L}{D} \ll 1 \text{ and } \dfrac{D\bar{\Gamma}_\mu}{v_w^2} \ll 1, \\ \dfrac{6D}{v_w L}\exp\left[-\dfrac{v_w}{D}\left(z - \dfrac{L}{2}\right)\right], & \dfrac{v_w L}{D} \gg 1 \text{ and } \dfrac{D\bar{\Gamma}_\mu}{v_w^2} \ll 1, \\ \dfrac{1}{2}\sqrt{\dfrac{\bar{\Gamma}_\mu}{D}}L\exp\left[-\sqrt{\dfrac{\bar{\Gamma}_\mu}{D}}\left(z - \dfrac{L}{2}\right)\right], & \sqrt{\dfrac{\bar{\Gamma}_\mu}{D}}L \ll 1 \text{ and } \dfrac{D\bar{\Gamma}_\mu}{v_w^2} \gg 1, \\ \dfrac{3}{L}\sqrt{\dfrac{D}{\bar{\Gamma}_\mu}}\exp\left[-\sqrt{\dfrac{\bar{\Gamma}_\mu}{D}}\left(z - \dfrac{L}{2}\right)\right], & \sqrt{\dfrac{\bar{\Gamma}_\mu}{D}}L \gg 1 \text{ and } \dfrac{D\bar{\Gamma}_\mu}{v_w^2} \ll 1. \end{cases} \tag{58}$$

This again shows the same results in each case. The only difference is the numerical factor that comes from averaging the profile over the wall, which is precisely what we anticipated, since $F_0/6 = \langle Av_w(Zm^2/T_0^3)\rangle$.

Using (48), we now finally calculate the baryon asymmetry in its standard form and find

$$\frac{n_B}{s} = \frac{4}{g_*}\kappa_s \alpha_w^4 \int \frac{g_A Zm^2}{T_0^2}dz \begin{cases} 1 \text{ if } v_w^2 > \Gamma_{ss} D \approx \dfrac{\kappa_{ss}}{6}, \\ \frac{1}{2} \text{ if } v_w^2 < \dfrac{\kappa_{ss}}{7} \text{ and } \sqrt{\dfrac{\Gamma_{ss}}{D}}L \approx \dfrac{\sqrt{\kappa_{ss}}LT}{14} < 1, \\ \dfrac{\eta D}{\Gamma_{ss}L^2} \text{ if } v_w^2 < \dfrac{\kappa_{ss}}{7} \text{ and } \dfrac{\sqrt{\kappa_{ss}}LT}{14} > 1, \end{cases} \tag{59}$$

where $s = (2\pi^2/45)g_*T^3$ is the entropy density of the universe, g_* is the number of relativistic degrees of freedom, and L is the thickness of the wall. η is a geometrical factor, which must be calculated for the particular wall profile (1 for ramp and 3 for bell). In all cases we have assumed $\Gamma_s \ll v_w^2/D$; in the case of a wall moving sufficiently slowly that this condition is violated, one would recover $n_B \propto v_w$, as expected. Recall that these results are derived under the assumption that the strong sphaleron is the dominant decay process everywhere. Other cases can be treated using the more general form of (46).

This expression is remarkably simple. Most strikingly L, v_w and D all cancel out in the answer in the most interesting (and quite plausible) regimes. For typical "slow thick wall" parameters values, e.g., $L \sim 10/T$, $v_w \sim 0.1$, $\kappa_{ss} \sim 0.1-1$, and $m_t \sim T$, the conditions for our derivation hold. The result is $\approx 2\times 10^{-2}\kappa_s\alpha_w^4(m/T)^2\Delta\theta \approx 2\times 10^{-8}\kappa_s\Delta\theta$, where $\Delta\theta \equiv m_t^{-2}\int m_t(z)^2 g_A Z\,dz$ is a measure of the CP-violating condensate on the wall.

The magnitude of $\Delta\theta$ depends on the precise profile of the wall, with the greatest effect occurring (in the two doublet theory) if the phase θ rolls fastest where the mass is large. In two-doublet theories it will have the same sign on every bubble in a way determined by the effective potential, and can be $O(1)$ consistently with measurements of CP violation. In the case of the standard model Z condensate this factor will contain a suppression (potentially many orders of magnitude) depending on exactly how one sign of the condensate comes to dominate over the other. A full treatment of this case is required, which goes beyond the scope of this paper [13].

B. Local spontaneous baryogenesis

In the preceding section we have concentrated primarily on the chemical potential fluctuations in front of the wall where the sphaleron rate is unsuppressed. This clearly dominates baryon production in the case of efficient transport $v_wL/D < 1$. In the case of inefficient transport (when the wall is very thick and slow) so that $v_wL/D \gg 1$, the nonlocal baryogenesis will be suppressed by $\sim D/v_wL$, and local baryogenesis may dominate. We analyze this case now to relate our treatment to that in the literature (in particular, to CKN's work [8]) prior to [10], in which the potential importance of transport in the plasma was noted.

When we combine the first two equations in (46) and ignore transport ($D = 0$), we obtain

$$v_w\mu_\Delta'' - (\Gamma_f+\Gamma_{ss})\mu_\Delta' + \frac{\Gamma_f\Gamma_{ss}}{v_w}\left(1-\frac{1}{N_f}\right)\mu_\Delta = -2N_c\Gamma_f v_w g_A Z'\,. \quad (60)$$

The force term source drops out in this limit simply because, in order to induce perturbations, particles must move in response to the force (and $D = 0$ "freezes" the particles). The case of the perturbations induced by the second source terms on the right-hand side of (46) is quite different. The effect of the field Z is local–it creates a perturbation at the point at which it is turned on by changing the interaction rates of hypercharge violating processes.

For comparison with the previous literature, it is instructive to consider the following cases in which the solutions to this equation can be read off simply.

Case 1. $\Gamma_f^{-1} \ll L/v_w \ll \Gamma_{ss}^{-1}$ for which

$$\mu_\Delta = 2N_c v_w g_A Z \quad (61)$$

to leading order in Γ_{ss}/Γ_f.

Case 2. $\Gamma_{ss}^{-1}, \Gamma_f^{-1} \ll L/v_w$ for which

$$\mu_\Delta = -2\frac{N_c}{1-N_f^{-1}}\frac{v_w}{\Gamma_{ss}}v_w g_A Z'\,. \quad (62)$$

Here we ignore the homogeneous solutions, which simply describe how the perturbations induced on the wall decay away behind the wall.

The first case gives us what would be obtained by finding the local equilibrium subject to the constraints imposed by the interactions locally, neglecting strong sphalerons. This is precisely the limit calculated by CKN in [8], albeit with a fermionic hypercharge in place of v_wZ and correspondingly a fermionic hypercharge violating process in place of Γ_f. The requirement $\Gamma_f^{-1} \ll L/v_w$ is just the condition that the interaction time for the hypercharge-violating process be short in comparison to the time of passage of the wall, a requirement imposed by CKN on the fastest fermionic hypercharge-violating process.

From the second case we see that if one takes $\Gamma_{ss} \to \infty$, i.e., puts the strong sphalerons into equilibrium, the result is zero. This is a simple way of seeing the result obtained by Giudice and Shaposhnikov in [14]. The result (62) tells us how to calculate corrections to this constrained local equilibrium calculation, keeping the constraints but taking the rates to be finite, and gives what one might guess: The result is approximately equal to the equilibrium result of (61) with an additional suppression $v_w/\Gamma_{ss}L$.

These formulas also show, as remarked upon earlier and pointed out by Dine and Thomas in [9], that the perturbation is not well modeled by a fermionic hypercharge potential, but is it a potential for total hypercharge? In the rest frame of the plasma, with our assumption of a stationary wall profile, the time component of $\tilde{Z}_\mu$ is v_wZ, but one must be careful about the conclusion that one simply replaces v_wZ by whatever this time component is. One evident problem is that one loses the explicit v_w dependence, as such a potential can, in principle, be nonzero with the wall at rest, and the result when $v_w \to 0$ is then nonzero. The problem is exemplified in CKN's calculation of spontaneous baryogenesis [12], which incorporates the effect of transport through a diffusion equation, in which only the time component of $\tilde{Z}_\mu$ appears. However, if we consider the case in which *only* the time component $\tilde{Z}_\mu$ is nonzero, their diffusion equation does not approach the correct thermal equilib-

rium as $v_w \to 0$. To recover this must include the force term, which results in a net overdensity in proportion to $\tilde{Z}_0$. In general, a correct treatment should include both space and time components of the gauge field and the corresponding force terms. In our case, where the field configuration is assumed static in the wall frame, one can work in this frame, and, in this case, the only nonzero component is the *spatial* z component, while the time component plays no role. We will not compute, in this case, the baryon asymmetry, as it involves making specific assumptions about how the electroweak sphaleron rate behaves on the wall. We concentrate instead on the nonlocal variant of this mechanism.

This brings us to one final remark. When the transition proceeds, as we have assumed, by bubble nucleation, $\tilde{Z}_\mu$ is a spacelike vector if we take the wall profile to be stationary. The one case in which it can be modeled consistently as a timelike total hypercharge potential is when the transition occurs by spinodal decomposition, where the Higgs-boson fields all roll together in the same way everywhere in space. Going back to our dispersion relation in Sec. II for this case, we would follow through our deviations in the same way. We would need to redefine the chemical potential by $g_A\tilde{Z}_0$ and, because of the spatial homogeneity, would find no force term. For the same reason, we would discard the spatial gradients and, with a certain assumption about how the transition proceeds, the time derivatives too. We would arrive at (61) above with $v_w Z$ replaced by $\tilde{Z}_0$.

C. Nonlocal spontaneous baryogenesis

We now turn to the case where this local effect is turned into a nonlocal one by the effects of transport. Perturbations can then be generated in front of the wall where the sphaleron rate is unsuppressed, in contrast to the local effect, which operates in the region where B violation is VEV squared suppressed (see, e.g., [12]).

We turn again to (49), again assuming Γ_{ss} to be the dominant decay process, taking the second source term and the ramp *Ansatz*:

$$\frac{\Gamma_f Z}{T_0} = \begin{cases} -\dfrac{\Gamma_0 Z_0}{T_0}\left(\dfrac{z-\frac{L}{2}}{L}\right), & -\dfrac{L}{2} < z < \dfrac{L}{2}, \\ 0, \ \text{otherwise.} \end{cases} \tag{63}$$

The VEV squared dependence in the rate is absorbed in the *Ansatz*. With this *Ansatz*, $\bar{\mu}_\Delta$ is then continuous everywhere, but the equation is not homogeneous.

The particular solution for this *Ansatz* is

$$\frac{\bar{\mu}_\Delta}{T_0} = \begin{cases} -v_w \dfrac{\Gamma_\mu}{\bar{\Gamma}_\mu}\dfrac{g_A Z_0}{T_0}\left(\dfrac{z-\frac{L}{2}}{L} + \dfrac{v_w}{\bar{\Gamma}_\mu L}\right), & -\dfrac{L}{2} < z < \dfrac{L}{2}, \\ 0, \ \text{otherwise,} \end{cases} \tag{64}$$

and the solution in front of the wall

$$-2N_c v_w \frac{\Gamma_\mu}{\bar{\Gamma}_\mu}\frac{g_A Z_0}{T_0}\frac{1}{(\lambda_f+\lambda_b)L}\left[\left(-1+\frac{\lambda_b}{\lambda_d^0}\right)+\left(1-\frac{\lambda_b}{\lambda_d^0}+\lambda_b L\right)e^{-\lambda_f L}\right]e^{-\lambda_f(z-L/2)} \tag{65}$$

using the same conventions again as in (52), and $\lambda_d^0 = \bar{\Gamma}_\mu / v_w$.

Again we simplify this in various limits to

$$+2N_c v_w \frac{\Gamma_\mu}{\bar{\Gamma}_\mu}\frac{g_A Z_0}{T_0}\begin{cases} -\dfrac{1}{2}\dfrac{v_w L}{D}\left(\dfrac{D\bar{\Gamma}_\mu}{v_w^2}\right)\exp\left[-\dfrac{v_w}{D}\left(z-\dfrac{L}{2}\right)\right], & \dfrac{v_w L}{D} \ll 1 \ \text{and} \ \dfrac{d\bar{\Gamma}_\mu}{v_w^2} \ll 1, \\ \dfrac{D}{v_w L}\left(\dfrac{D\bar{\Gamma}_\mu}{v_w^2}\right)\exp\left[-\dfrac{v_w}{D}\left(z-\dfrac{L}{2}\right)\right], & \dfrac{v_w L}{D} \gg 1 \ \text{and} \ \dfrac{d\bar{\Gamma}_\mu}{v_w^2} \ll 1, \\ \dfrac{1}{4}\sqrt{\dfrac{\bar{\Gamma}_\mu}{D}}L\exp\left[-\sqrt{\dfrac{\bar{\Gamma}_\mu}{D}}\left(z-\dfrac{L}{2}\right)\right], & \sqrt{\dfrac{\bar{\Gamma}_\mu}{D}}L \ll 1 \ \text{and} \ \dfrac{D\bar{\Gamma}_\mu}{v_w^2} \gg 1, \\ \dfrac{1}{2L}\sqrt{\dfrac{D}{\bar{\Gamma}_\mu}}\exp\left[-\sqrt{\dfrac{\bar{\Gamma}_\mu}{D}}\left(z-\dfrac{L}{2}\right)\right], & \sqrt{\dfrac{\bar{\Gamma}_\mu}{D}}L \gg 1 \ \text{and} \ \dfrac{D\bar{\Gamma}_\mu}{v_w^2} \gg 1. \end{cases} \tag{66}$$

These solutions are very similar to those in the case of the force, the amplitude being of the form of the amplitude of a "static" solution (61) on the wall multiplied by a factor that depends on the relative importance of decay and diffusion. The static solution in this case is attained in the limit that there is no transport and the decay processes are turned on.

In contrast, the solution (36) for the force is reached when transport is perfect and the decay processes are turned off. For the "spontaneous" effect, we see that as $D \to 0$ the amplitude in front of the wall vanishes rapidly ($\sim D^2$).

As $D \to \infty$ the amplitude goes as $1/\sqrt{D}$, but the tail integrates to give exactly half the solution (61), however, in this case not with the opposite sign. The arguments that we use to explain the sign in the case of the force do not apply as they rested on (40). In the spontaneous result the sign is, in all but the first case, the same as that of the static solution. What is happening is that the overdensity, which the local process creates, diffuses out to the region in front of the wall. Only in the first case, where the transport is much more efficient than the decay, do particles

diffuse in to "cancel" the density on the wall.

The baryon to entropy ratio can again be calculated. We find precisely the same expressions in (59) but with the replacement

$$\int \frac{g_A Z m^2}{T_0^2} dz \to \frac{b}{2c} \int \frac{\Gamma_f g_A Z}{\Gamma_{ss}} dz \begin{cases} \frac{D\bar{\Gamma}_{ss}}{v_w^2} \approx \frac{D\kappa_{ss}}{7v_w^2}, & v_w^2 \gg \frac{\kappa_{ss}}{7}, \\ 1, & v_w^2 \ll \frac{\kappa_{ss}}{7}. \end{cases} \tag{67}$$

Using Γ_f and Γ_{ss} from (47) so that $\Gamma_f/\Gamma_{ss} \simeq 0.4(m_t/T)^2/\kappa_{ss}$, this result is seen to be equal to the force result multiplied by $\simeq 1/(50\kappa_{ss}\alpha_s^2) \simeq 1/\kappa_{ss}$. (This is valid for $v_w^2 \ll \kappa_{ss}/7$ and, as we assumed, $\Gamma_{ss} \gg \Gamma_f$.) The final result is that the two effects have quite different parametric dependence but appear to be roughly of the same order of magnitude.

A striking difference between the classical force effect and the spontaneous baryogenesis effect is in the dependence on the strong sphaleron rate. In the latter there is an inverse dependence on the sphaleron rate for a sufficiently large κ_{ss}. This dependence has been noted by CKN in their numerical study [12]. In contrast, the force sourced result is not suppressed by the strong sphalerons if $\sqrt{\kappa_{ss}}LT/14 < 1$.

VII. COMPARISON OF THIN- AND THICK-WALL REGIMES

It is interesting to compare the results in this paper with those in [6], where we considered the case of baryogenesis produced by reflection off a thin wall. The two calculations are most easily compared by looking at the version of the fluid equations (46). Once we established that the thermal fluctuations were unimportant, we were able to reduce the system to a diffusion equation precisely analogous to that in [6] but including a force term that extends over a finite region of space, the wall, where we before had the derivative of a δ function, modeling the injected flux:

$$\xi J_0 \delta \to \frac{D}{b} F(z) . \tag{68}$$

In the classical force case, integrating the right-hand side gives zero because the force is derived from a potential. Unlike the injected case, the effect of the classical force vanishes as the wall thickness is taken to zero. This is because the force simply speeds up and slows down particles that pass over it. We have not included the effect of the force as a reflecting barrier on low momentum states, since we neglected the effect of the "flow" of one branch of the dispersion relation into the other at low momentum. If we include this we should obtain in the thin-wall limit what one would calculate for the reflected flux in the WKB limit. The quantum-mechanical reflection we cannot of course recover. To compare the magnitude of the classical force effect with the WKB reflection effect, we take the ratio of the amplitudes of the diffusion tails at the front of the wall. Doing this, we find, neglecting decay and assuming efficient transport,

$$\frac{\mu_{\rm refl}}{\mu_{\rm force}} \sim \frac{\xi}{D} LT \frac{D}{v_w L} \eta . \tag{69}$$

The most striking result is the very different parametric dependence.

The effect of introducing a decay term, in particular, because of strong sphalerons, is quite different in the two cases. In our thin-wall calculations [6] the suppression that resulted was $v_w/\sqrt{\Gamma_{ss}D}$ for $v_w^2/\Gamma_{ss}D \ll 1$, and this same suppression is seen in the nonlocal spontaneous effect. In the case of the classical force this suppression (which comes from the shortening of the diffusion tail in front of the wall) is compensated for by an increase in amplitude until Γ_{ss} enters the regime $\sqrt{\Gamma_{ss}/D}L > 1$. An explanation may be found from the equation for $\bar{\mu}_\Delta$, Eq. (46). Dropping both Γ_f terms and integrating once, one finds that the integral of $\bar{\mu}_\Delta$ over all space must be zero. What the condition $\sqrt{\Gamma_{ss}/D}L < 1$ means is that strong sphalerons have little effect on the wall, but, because $\int \mu_\Delta = 0$, the compensating tail in front of the wall is also unaffected. No analogous conservation law holds in the spontaneous baryogenesis effect because the whole effect is driven by a decay process (Γ_f) and strong sphaleron suppression occurs.

VIII. CONCLUSION

In this paper we have developed a systematic procedure to describe the perturbations produced by a CP-violating bubble wall moving through the plasma. We have shown how a Boltzmann equation can be used to describe the dynamics of thermal particles in the plasma when scattering processes are important. We now conclude with several remarks.

(i) The treatment relies on a WKB approximation which is good for most, but not all modes in the plasma. We have in particular ignored the effect of the low momentum modes. A full treatment including these modes remains an open problem—for recent attempts see [15].

(ii) We have neglected the effect of screening. The effects of the long-range fields may be incorporated through the appropriate terms in the Boltzmann and fluid equations. We have not done this, as it greatly complicates our analysis by coupling all species. However, in Sec. VII of [6] we discuss this issue in some detail. As illustrated by a simple model calculation of screening by quarks and leptons presented there, we do not expect that the effects of screening would alter our final results by a factor very different from unity.

(iii) There are many improvements and refinements of

our calculation possible. The Boltzmann equation is, in principle, soluble without any truncation, and certainly there are other approximations that can be used.

(iv) One caveat must be added to our justification of the neglect of the Higgs particles in the determination of the perturbations driving baryogenesis. By dropping the Higgs particles we are assuming that they themselves are not significantly perturbed by a force term. In the thin-wall case we also assumed that there was no injected flux in Higgs particles. This is not justified, as the dynamics of the Higgs particles are likely to be nontrivial in the background of a changing VEV. It is quite conceivable that such an effect could be important.

(v) The methods we have developed should be useful in approaching the problem of the determination of the wall velocity and backreaction on the wall because of reflection. In particular, we derived a set of force terms caused by the mass, which we did not make use of in the calculation reported here.

(vi) An important outstanding problem is to relate the techniques developed here to some formal field theoretic methods such as those used in [16] and more recently in [17].

ACKNOWLEDGMENTS

M.J. was supported by the Charlotte Elizabeth Procter Foundation, and the work of T.P. and N.T. was partially supported by NSF Contract No. PHY90-21984 and the David and Lucile Packard Foundation. We thank the Isaac Newton Institute, Cambridge for hospitality during the completion of the manuscript.

APPENDIX A: COLLISION INTEGRALS FOR BOSON EXCHANGE[2]

We consider first the contribution to the collision integrals in the fluid equations, which come from the t-channel gauge boson exchange processes shown[3] in Fig. 2. We will treat not just the quarks but also the right- and left-handed leptons, primarily because it is interesting to compare our result for the diffusion constant with those obtained with our previous method in [6].

When we integrate the Boltzmann equation as described in the text over $\int \not{d}^3p$, $\int p_0 \not{d}^3p$, and $\int p_z \not{d}^3p$ there are six integrals we need to evaluate:

$$\int_{p,k,p',k'} f_p(1-f_p)f_k(1-f_k)|\mathcal{M}|^2(2\pi)^4\delta^4(p+k-p'-k')(p_0-p_0')\times\begin{Bmatrix}1\\ p_0,\\ p_z\end{Bmatrix}$$
$$\int_{p,k,p',k'} f_p(1-f_p)f_k(1-f_k)|\mathcal{M}|^2(2\pi)^4\delta^4(p+k-p'-k')(p_z-p_z')\times\begin{Bmatrix}1\\ p_0,\\ p_z\end{Bmatrix} \tag{A1}$$

where we have ignored the higher-order terms in the perturbations δT, $\bar{v}$, and μ so that fermion population densities (in the plasma frame) are $f_{p_i} = 1/[1+\exp(p_i^0/T_0)]$, $p_i = \{p,k,p',k'\}$.

For the gluon exchange process the scattering amplitude is

$$|\mathcal{M}_q|^2 = A_q\frac{s^2+u^2}{(t-m_g^2)^2}, \tag{A2}$$

where $A_q = 32g_s^4$, $t=(p-p')^2 \simeq -2p\cdot p'$, $s=(p+k)^2\simeq -2p\cdot k$, $u=(p-k')^2\simeq -2p\cdot k'$, g_s is the strong-coupling constant and m_g is the thermal gluon mass. Note that here and in the following we neglect masses of the particles at legs of the diagram. Since typical scattering particles are thermal $p\sim k\sim T$, including them would introduce mass-squared corrections to our collision integrals, which we can safely neglect. For the SU(2) and U(1) boson exchange diagrams for leptons,

$$|\mathcal{M}_W|^2 = A_W\frac{s^2}{(t-m_W^2)^2},\quad |\mathcal{M}_B|^2 = A_B\frac{s^2}{(t-m_B^2)^2}, \tag{A3}$$

where $A_W = 36g_W^4$, $A_B = 78g_w^4\tan^4\theta_w$, g_w the weak-coupling constant, θ_w the Weinberg angle, and m_W and m_B the thermal masses of the SU(2) and U(1) gauge bosons, respectively. These amplitudes include the counting over all the

[2]We thank Guy Moore for pointing out an error in an earlier version of this appendix.

[3]In this paper we do not calculate all of the t channel tree-level diagrams that contribute to the diffusion constant. We refer the reader to [5], where this has been done systematically.

fermions and antifermions, which the given fermion can scatter off. Since the t-channel processes are dominated by the infrared exchange momenta, we have used the same approximation to the boson propagator as in Appendix C of [6]: We have assumed the exchange boson is Debye screened and hence the propagator is corrected by $t \to t - m^2$, where $m(T)$ is the corresponding Debye mass. This approximation is reasonable for longitudinal bosons, but for transverse bosons, since they are not Debye screened at the one-loop level, it underestimates the scattering rates.

To see that the first and fourth integral are zero we simply use the symmetry of the matrix element under exchange of initial and final momenta, i.e., $p \to p'$ and $k \to k'$.

Using parity invariance of the amplitudes ($\vec{p}_i \to -\vec{p}_i$), one can show that the third and fifth integrals are also zero. We are left with only two integrals, which we denote as I^0 (the *second* integral) and I^3 (the *sixth* integral), which can be written in a Lorentz-invariant form as

$$
\begin{aligned}
I^0 &= \int \frac{d^3p}{2p_0} \int \frac{d^3k}{2k_0} f_p f_k \iota^0, \quad I^3 = \int \frac{d^3p}{2p_0} \int \frac{d^3k}{2k_0} f_p f_k \iota^3 , \\
\iota^0 &= \int \frac{d^3p'}{2p'_0}(1-f_{p'}) \int \frac{d^3k'}{2k'_0}(1-f_{k'})|\mathcal{M}|^2(2\pi)^4\delta^4(p+k-p'-k')\frac{1}{2}[(p-p')\cdot u]^2 , \\
\iota^3 &= \int \frac{d^3p'}{2p'_0}(1-f_{p'}) \int \frac{d^3k'}{2k'_0}(1-f_{k'})|\mathcal{M}|^2(2\pi)^4\delta^4(p+k-p'-k')\frac{1}{6}[-t+\{(p-p')\cdot u\}^2] ,
\end{aligned}
\tag{A4}
$$

where u^μ is the plasma vector, which is in the plasma frame $u^\mu = (1,\vec{0})$, and $f_{p_i} = 1/[1+\exp(p_i\cdot u/T)]$ are the population densities. Dropping the Pauli blocking factors for the out-going states we can evaluate the integrals over p' and k' in the center-of-mass frame. In this frame $u^\mu = (\gamma,\gamma\vec{v})$, which can be written in terms of the plasma frame quantities as $\gamma = (p_0^{\rm pl}+k_0^{\rm pl})/\sqrt{s^{pl}}$, $\gamma\vec{v} = (\vec{p}^{pl}+\vec{k}^{pl})/\sqrt{s^{\rm pl}}$, $s^{\rm pl} = 2p^{\rm pl}\cdot k^{\rm pl}$. For convenience we choose the axes such that $\vec{p}$ is along the z axis, $\vec{p} = p(0,0,1)$; $\vec{v}$ has *zero* azimuthal angle, $\vec{v} = v(\sin\beta,0,\cos\beta)$; and $\vec{p}' = p'(\sin\theta'\cos\phi',\sin\theta'\sin\phi',\cos\theta')$. After some algebra, and keeping only the leading logarithm, which occurs for small θ', we get

$$
\begin{aligned}
\iota^0 &= \frac{A}{8\pi}(\gamma v p\sin\beta)^2 \ln\frac{4p^2}{m_g^2} , \\
3\iota^3 &= \frac{A}{8\pi}[(\gamma v p\sin\beta)^2 + 2p^2]\ln\frac{4p^2}{m_g^2} ,
\end{aligned}
\tag{A5}
$$

where $A = 2A_q$ for quarks and $A = A_W$, $A = A_B$ for the leptons. In order to recast this in a Lorentz-invariant form, note that the Lorentz scalars we can construct from u^μ, p^μ, and k^μ are $u\cdot p$, $u\cdot k$, and $p\cdot k$ (since $p\cdot p \simeq 0$, $k\cdot k \simeq 0$, and $u\cdot u = 1$). The unique solution is $(\gamma v p\sin\beta)^2 = (u\cdot p)(u\cdot k) - (p\cdot k)/2$, so that we have

$$
\begin{aligned}
\iota^0 &= \frac{A}{8\pi}\left[(u\cdot p)(u\cdot k) - \frac{p\cdot k}{2}\right]\ln\frac{2p\cdot k}{m_g^2} , \\
3\iota^3 &= \frac{A}{8\pi}\left[(u\cdot p)(u\cdot k) + \frac{p\cdot k}{2}\right]\ln\frac{2p\cdot k}{m^2} .
\end{aligned}
\tag{A6}
$$

It is now possible to do the remaining integrations using the approximation $\int f_x x^n \ln x\, dx \approx \ln(n+1)\int f_x x^n\, dx$, $f_x = (1+\exp x)^{-1}$; we find

$$
I^0 = I^3 = \frac{A}{1024\pi^5} 9\zeta_3^2 \ln\frac{36T^2}{m^2} T^6 . \tag{A7}
$$

Now going back to the definitions of Γ_T and Γ_v in (21) and (19) we have

$$
\Gamma_T = \frac{1}{4\rho_0 T_0} I^0, \quad \Gamma_v = \frac{3}{4\rho_0 T_0} I^3 , \tag{A8}
$$

where $\rho_0 = (21/8\pi^2)\zeta_4 T_0^4$. For the quarks, this gives, when we use $m_g^2 = 8\pi\alpha_s T_0^2 \approx 3.6 T_0^2$, as described in Appendix A of [6] for $\alpha_s = \frac{1}{7}$ at $T_0 \sim 100$ GeV,

$$
\Gamma_v = 3\Gamma_T = \frac{18\zeta_3^2}{7\zeta_4\pi}\alpha_s^2 \ln\frac{9}{2\pi\alpha_s} T_0 \approx \frac{T_0}{20} . \tag{A9}
$$

Using the relation $D = b/3a\Gamma_v$ from (22), this gives us the quark diffusion constant

$$
D_q^{-1} = \frac{8\zeta_2}{\pi}\alpha_s^2 \ln\frac{9}{2\pi\alpha_w} T_0 \approx \frac{T_0}{5} . \tag{A10}
$$

For the leptons we calculate

$$
\begin{aligned}
D_W^{-1} &= \frac{9\zeta_2}{2\pi}\alpha_w^2 \ln\frac{27}{5\pi\alpha_w} T_0 \approx \frac{T_0}{100} , \\
D_B^{-1} &= \frac{39\zeta_2}{4\pi}\alpha_w^2 \tan^4\theta_W \ln\frac{27}{\pi\alpha_w\tan^2\theta_W} T_0 \approx \frac{T_0}{290} ,
\end{aligned}
\tag{A11}
$$

where we used $m_B^2 = (4\pi/3)\alpha_w \tan^2\theta_W T_0^2 \simeq 0.04 T_0^2$ and $m_W^2 = (20\pi/3)\alpha_w\tan^2 T_0^2 \simeq 0.7 T_0^2$ and taking $\alpha_w = \frac{1}{30}$ and $\sin^2\theta_W = 0.23$.

These values for the diffusion constants agree very well with the values we obtained in Appendix A of [6]. The methods employed differ in that the first allowed a more general perturbation to the phase space density, but required an assumption about the near equality of the energy of ingoing and outgoing scattered particles. The method presented here is based on a more restrictive form for the distribution function but involves no additional approximations.

APPENDIX B: COLLISION INTEGRALS FOR DECAY PROCESSES

In this appendix we evaluate the gluon exchange helicity-flip rate, which dominates the hypercharge-

violating interactions. The relevant Feynman diagram is shown in Fig. 2. The top–Higgs-boson helicity-flip processes (hypercharge-violating Higgs exchange and Higgs absorption or emission) are slower because there are fewer particles to scatter off.

The rate for a top quark of helicity λ to scatter into one of helicity λ' is

$$\Gamma_{\lambda\to\lambda'}| = \frac{12}{T^3}\int \frac{d^3p}{2p_0} f_0(p_0/T)\frac{d^3k}{2k_0} f_0(k_0/T)\mathcal{I}_f\,, \tag{B1}$$

$$\mathcal{I}_f = \int \frac{d^3p'}{2p'_0}\frac{d^3k'}{2k'_0}\,\delta^4(p+k-p'-k')|\mathcal{M}_{\lambda\to\lambda'}|^2\,,$$

on the wall where particles acquire a mass. The factor $12/T^3 = 1/3n_0a$ is in accord with the rate definition Γ_f in the diffusion equations (46). Even though the masses are spatially dependent, for our purposes it is sufficient to evaluate the rate assuming a constant mass. The corrections to this approximation are of order $l\nabla m$, where $l \sim 1/M_g$ is the Debye screening length of the gluon so that $l|\nabla m|/m \sim 1/g_sTL \ll 1$. In (B1) we consider an in-going fermion with mass m_1 momentum and helicity $\{p,\lambda\}$, which scatters off a fermion m_2, k (with arbitrary helicity) into $\{p',\lambda'\}, k'$ with the appropriate spin-dependent scattering amplitude $\mathcal{M}_{\lambda\to\lambda'}$. The notation we use in (B1) is familiar to the reader: $n_0 = 3\zeta_3T^3/4\pi^2$, $\zeta_3 = 1.202$, $f_0(x) = 1/(\exp x + 1)$, $d^3k \equiv d^3k/(2\pi)^3$. We ignore Pauli blocking factors.

In order to evaluate $|\mathcal{M}_{\lambda\to\lambda'}|^2$ we define, following, e.g., [18], the spin-four vector as

$$s^\mu = \frac{2\lambda}{m}\left(|\vec{p}|, p_0\frac{\vec{p}}{|\vec{p}|}\right),\quad \lambda = \pm\frac{1}{2}\,, \tag{B2}$$

where λ is the helicity, so that $s\cdot p = 0$ and $s\cdot s = -1$. The helicity projection operators for a massive spin-$\frac{1}{2}$ particle eigenspinor $u(p,\lambda)$ are

$$u(p,\lambda)\bar{u}(p,\lambda) = \tfrac{1}{2}(1+\gamma_5\,\not{s})(\not{p}+m) \tag{B3}$$

and similarly for antiparticles.

The scattering amplitude squared reads

$$|\mathcal{M}_{\lambda\to\lambda'|^2} = \frac{2A_s}{[(p-p')^2 - M_g^2]^2}\frac{1}{16}T_1\cdot T_2\,,$$
$$T_1^{\nu\mu} = \mathrm{Tr}[(\not{k}+m)\gamma^\nu(\not{k}'+m)\gamma^\mu]\,, \tag{B4}$$
$$T_{2\nu\mu} = \mathrm{Tr}\{(\not{p}+m)\gamma_\nu\tfrac{1}{2}[1+\gamma_5\,\not{s}(p',\lambda')]$$
$$\times(\not{p}'+m)\gamma_\mu\tfrac{1}{2}[1+\gamma_5\,\not{s}(p,\lambda)]\}\,,$$

where $A_s = 32g_3^4 = 512\pi^2\alpha_s^2$ ($\alpha_s = g_3^2/4\pi = 1/7$) includes the 12 quarks and antiquarks that a quark can scatter off via the gluon exchange. Rather than evaluating $|\mathcal{M}_{\lambda\to\lambda'}|^2$ for each pair $\{\lambda,\lambda'\}$, we can define the helicity-flip amplitude

$$|\mathcal{M}_-|^2 = \tfrac{1}{2}\sum_{\lambda'=-\lambda}|\mathcal{M}_{\lambda\to\lambda'}|^2 \tag{B5}$$

and the no-flip amplitude

$$|\mathcal{M}_+|^2 = \tfrac{1}{2}\sum_{\lambda'=\lambda}|\mathcal{M}_{\lambda\to\lambda'}|^2\,, \tag{B6}$$

which simplifies the problem considerably. We still have to plough through rather lengthy algebra to arrive at an expression for $T_1\cdot T_2\pm$:

$$\begin{aligned}\frac{1}{16}T_1\cdot T_{2\pm} = \frac{1}{2}\sum_{\lambda'=\pm\lambda}\frac{1}{16}T_1\cdot T_2 &= (p\cdot kp'\cdot k' + p\cdot k'p'\cdot k - m_1^2k\cdot k' - m_2^2p\cdot p' + 2m_1^2m_2^2)\\ &\pm\frac{1}{2}\sum_{\lambda'=\lambda}[-s\cdot s'(p\cdot kp'\cdot k' + p\cdot k'p'\cdot k - p\cdot p'k\cdot k')\\ &-p\cdot p'(k\cdot sk'\cdot s' + k\cdot s'k'\cdot s) + p\cdot kp'\cdot sk'\cdot s'\\ &+p\cdot k'p'\cdot sk\cdot s' + p'\cdot kp\cdot s'k'\cdot s + p'\cdot k'k\cdot sp\cdot s' - k\cdot k'p\cdot s'p'\cdot s\\ &+m_1^2(k\cdot sk'\cdot s' + k\cdot s'k'\cdot s - m_2^2s\cdot s')]\,,\end{aligned} \tag{B7}$$

where $s_\mu = s_\mu(p,\lambda)$ and $s'_\mu = s_\mu(p',\lambda')$.

Since this form is Lorentz invariant, the integration over the out-going momenta p' and k' is rather straightforward in the center-of-mass frame: $\vec{p}+\vec{k} = 0 = \vec{p}'+\vec{k}'$. To leading order in m_1^2 we obtain

$$\mathcal{I}_- = \frac{A_s}{8\pi}\frac{m_1^2}{p\cdot k}\ln\left[1+\frac{2p\cdot k}{M_g^2}\right]\,,$$
$$\mathcal{I}_+ = \frac{A_s}{2\pi}\frac{p\cdot k}{M_g^2} \tag{B8}$$

with the gluon thermal mass squared $M_g^2 = 8\pi\alpha_sT^2$.

We can now integrate both $\mathcal{I}_-$ (in the leading logarithm approximation as explained in Appendix B of [6]) and $\mathcal{I}_+$ according to (B1) to obtain the helicity-flip rate Γ_- and the no-flip rate Γ_+:

$$\Gamma_f = \Gamma_- = \frac{24\ln^2 2}{\pi^3}\frac{m_1^2}{T^2}\alpha_s^2\iota T\,,$$
$$\Gamma_+ = \frac{54\zeta_3^2}{\pi^4}\alpha_sT\,, \tag{B9}$$

where

$$\iota = \int_0^2 (dz/z)\ln(1+x_1^2z/2\pi\alpha_s)$$
$$\simeq \zeta_2 + (1/2)\ln^2(x_1^2/\pi\alpha_s) - \pi\alpha_s/x_1^2 \simeq 2.5$$

is the angular integral ($z = p \cdot k/pk$), which is approximately unity; $x_1 \sim 1.3$ is the value of the momentum p/T at which the momentum integrals in (B1) peak.

We use this estimate of Γ_f in Sec. VI. Using the same method one could evaluate the helicity-flip W- and B-exchange processes relevant for the leptons. However, since our main focus in this work is on top-quark-mediated baryogenesis, we shall not do so here.

APPENDIX C: FINITE-TEMPERATURE DISPERSION RELATION

In this appendix we follow Appendix B of [6] to arrive at a finite-temperature Dirac equation in momentum space. In the presence of a Z field condensate it is convenient to write the equation in terms of 2×2 chiral spinors in the plasma frame

$$[(E - g_A Z_0 + c_R) - \vec{\sigma} \cdot (\vec{P} - g_A \vec{Z})]\Psi_R + m_R \Psi_L = 0\,,$$
$$m_L \Psi_R + [(E + g_A Z_0 + c_L) + \vec{\sigma} \cdot (\vec{P} + g_A \vec{Z})]\Psi_L = 0\,, \tag{C1}$$

where the notation is that of [6]. We will consider a planar wall moving in the positive z direction with velocity v_w with a pure gauge condensate $Z^\mu = (Z_0, 0, 0, Z_z)(z)$ so that $Z_0 = -v_w Z_z$. The dispersion relation we require is obtained by setting the determinant of (90) to *zero*:

$$[(E+c)^2 - \vec{P}^2 - m_T^2 - (g_A Z_0 + \tfrac{1}{2}\Delta c)^2 + g_A^2 Z_z^2]^2 = 4\vec{P}^2 (g_A Z_0 + \tfrac{1}{2}\Delta c)^2 + 4 g_A^2 Z_z^2 [(E+c)^2 - \vec{P}_\perp^2] - 8 P_z g_A Z_z (E+c)(g_A Z_0 + \tfrac{1}{2}\Delta c)\,, \tag{C2}$$

where we have defined

$$c = \frac{c_R + c_L}{2}, \quad \Delta c = c_L - c_R, \quad m_T^2 = \frac{m^2}{(1+a_L)(1+a_R)}\,. \tag{C3}$$

The dispersion relation for antiparticles is obtained by the replacement $P_z \to -P_z$ and $Z_0 \to -Z_0$ (recall that Z_z is even under CP). In the limit when both $Z_0, Z_z \to 0$ we find, for particles,

$$(E+c)^2 = \left(|\vec{P}| \pm \frac{1}{2}\Delta c\right)^2 + m_T^2\,, \tag{C4}$$

which reduces in the high-momentum limit to $E^2 = P^2 + m_T^2 + 2M_{L,R}^2$.

A second case, which is easy to solve, is when $Z_z = 0$ and $Z_0 \neq 0$. This is relevant to the case of spinodal decomposition (second-order phase transition):

$$(E+c)^2 = [|\vec{P}| \mp (g_A Z_0 + \tfrac{1}{2}\Delta c)]^2 + m_T^2\,, \tag{C5}$$

which in the high-momentum limit simplifies to

$$E^2 = [|\vec{P}| \mp g_A Z_0]^2 + 2M_{L,R}^2 + m^2\,. \tag{C6}$$

Therefore, as long as $P \gg M_{L,R}$, the motion of a thermal excitation is not affected (to leading order) by the dispersive plasma effects. In a first-order phase transition this is not the relevant case, since Z^μ is spacelike; in the plasma frame, for example, $|Z_0/Z_z| = v_w$, so for slow walls it makes sense to neglect Z_0.

To make a detailed comparison with the free-particle case, we now proceed to a more systematic study of (C2) and rewrite it as

$$\begin{aligned} &\lambda = E + c\,,\\ &0 = \lambda^4 - 2[\vec{P}^2 + m_T^2 + g_A^2 Z_z^2 + (g_A Z_0 + \tfrac{1}{2}\Delta c)^2]\lambda^2 + 8 P_z g_A Z_z (g_Z Z_0 + \tfrac{1}{2}\Delta c)\lambda \\ &\quad + [\vec{P}^2 + m_T^2 - g_A^2 Z_z^2 + (g_A Z_0 + \tfrac{1}{2}\Delta c)^2]^2 + 4 m_T^2 [(g_A Z_0 + \tfrac{1}{2}\Delta c)^2 - g_A^2 Z_z^2] - 4 P_z^2 g_A^2 Z_z^2\,. \end{aligned} \tag{C7}$$

We now consider a weak Z field expansion of this equation and write the solution in the form

$$\lambda = \lambda_0 (1 + \epsilon)\,, \tag{C8}$$

where λ_0 is the solution of (C7) with linear term in λ neglected:

$$\begin{aligned} \lambda_0^2 &= e_0^2 \pm \sqrt{\Delta_0}\,,\\ e_0^2 &= \vec{P}^2 + m_T^2 + g_A^2 Z_z^2 + (g_A Z_0 + \tfrac{1}{2}\Delta c)^2\,,\\ \Delta_0 &= 4(\vec{P}^2 + g_A^2 Z_z^2)(g_A Z_0 + \tfrac{1}{2}\Delta c)^2 + 4 g_A^2 Z_z^2 (m_T^2 + P_z^2)\,. \end{aligned} \tag{C9}$$

The leading-order correction ϵ reads

$$\epsilon \simeq \mp \frac{2g_A Z_z P_z (g_A Z_0 + \frac{1}{2}\Delta c)}{\lambda_0 \sqrt{\Delta_0}}\,, \tag{C10}$$

where the signs coincide with (C9). In order to make more transparent what the dispersion relation (C8)–(C10) mean, we look at its high-momentum limit.

We now restrict ourselves to the case $Z_0 = 0$, $Z_z \neq 0$, which describes the case of a wall at rest in the plasma. Since for a stationary wall profile $Z_0 = -v_w Z_z$, we anticipate that this will be a good approximation for a sufficiently slow wall. There are two cases to consider depending on which term in the determinant Δ_0 in (98) dominates,

$$\begin{aligned} &\sqrt{\Delta_0} \simeq 2g_A Z_z \sqrt{P_z^2 + m_T^2} \quad \text{for } (\Delta c)^2 P^2 \ll 4 g_A Z_z^2 (P_z^2 + m^2)\,, \\ &\sqrt{\Delta_0} \simeq |\Delta c| P \simeq (M_L^2 - M_R^2)\frac{E}{P} \quad \text{for } (\Delta c)^2 P^2 \gg 4 g_A^2 Z_z^2 (P_z^2 + m^2)\,. \end{aligned} \tag{C11}$$

In the high-momentum limit these two cases reduce to a comparison between $M_L^2 - M_R^2$ and $2g_A Z P_z$. Since $M_L^2 - M_R^2 \approx \alpha_w T^2$ (see [6]), and we can write $2g_A Z \equiv \Theta_{CP}/L$, the two cases become approximately $\Theta_{CP} > \alpha_w LT$ and $\Theta_{CP} < \alpha_w LT$, which we, therefore, refer to as cases of strong and weak condensates, respectively. (Note that for a realistic wall thickness to be in the strong regime Θ_{CP} must be of order *unity*.)

In the first case the dispersion relations are

$$(E^{L,R} + c)^2 = P_\perp^2 + \left(\mathrm{sgn} P_z \sqrt{P_z^2 + m_T^2} \pm g_A Z_z\right)^2 + (\Delta c/2)^2 \mp (\Delta c/2)\frac{|P_z|}{\sqrt{P_z^2 + m_T^2}} 2(E^{L,R} + c) + (\Delta c/2)^2 \frac{P_z^2}{P_z^2 + m_T^2} \tag{C12}$$

$$(E^{\bar{L},\bar{R}} + c)^2 = P_\perp^2 + (\mathrm{sgn} P_z \sqrt{P_z^2 + m_T^2} \mp g_A Z_z)^2 + (\Delta c/2)^2 \mp (\Delta c/2)\frac{|P_z|}{\sqrt{P_z^2 + m_T^2}} 2(E^{\bar{L},\bar{R}} + c) + (\Delta c/2)^2 \frac{P_z^2}{P_z^2 + m_T^2}\,.$$

We have adopted here the notation used in the main text—labeling the WKB states by the chiral states they deform into in the symmetric phase. A careful inspection of these relationships in the high-momentum limit $P \gg M_{L,R}$, reveals that they reduce, to leading order in coupling constants, to the zero-temperature dispersion relations *plus* the finite-temperature mass $\sqrt{2}M_L$ for the left-handed particles and their antiparticles and $\sqrt{2}M_R$ for the right-handed particles and their antiparticles.

First we note that in the free case (when we set $T = 0$) Eq. (C12) precisely reproduces the dispersion relations we had in (4) and (5). Second, when $Z_z = 0$ we see that the effect of the thermal corrections is to split the left-handed and right-handed states (by an amount $\propto \Delta c$) but to leave the degeneracy of particles and antiparticles intact. Finally, and most important, we see that the corrections to the free dispersion relation are small, in this case $\Theta_{CP} > \alpha_w LT$, so that the analysis in the main text applies.

The second case of a weak condensate in (C11) gives dispersion relations

$$\begin{aligned} (E^{L,R} + c)^2 &= (P \mp \Delta c/2)^2 + m_T^2 \\ &\quad \pm 2 g_A Z_z \frac{P_z}{P}\sqrt{(P \mp \Delta c/2)^2 + m_T^2}\,, \end{aligned} \tag{C13}$$

$$\begin{aligned} (E^{\bar{L},\bar{R}} + c)^2 &= (P \pm \Delta c/2)^2 + m_T^2 \\ &\quad \mp 2 g_A Z_z \frac{P_z}{P}\sqrt{(P \pm \Delta c/2)^2 + m_T^2}\,. \end{aligned}$$

It is instructive to rewrite the first relation in the limit when $P \gg M_{L,R}$,

$$(E^{L,R})^2 \simeq P^2 + m^2 + 2M_{L,R}^2 \pm 2 g_A Z_z \frac{P_z}{P}\sqrt{P^2 + m^2}\,. \tag{C14}$$

When $m = 0$, there should be no physical effect because of the Z field, since it is then just pure gauge. We see that this is the case, since the dispersion relation can then be written $(E^{L,R} + c)^2 = (P' \mp \Delta c/2)^2$, where $P' = |\vec{P}'|$ and $\vec{P}' = (P_\perp, P_z \pm g_A Z_z)$ [compare this form with (C5)]. When $m \neq 0$, however, just as in the zero-temperature case, the dispersion relations (C13) lead to a nonzero acceleration: $\dot{v}_z = \mp \partial_z (g_A Z_z m^2)(P_z^3 E^3) - \partial_z m^2 / 2E^2$, where we have assumed that E and $P_\perp$ are conserved in the plasma frame, an approximation correct to leading order in v_w. Comparing this result with (8), we see that, in this second case of a weak condensate, the force term has the same form [$\propto \partial_z (g_A Z_z m^2)$] but a somewhat different momentum dependence. Corresponding corrections to the analysis presented in the text would be required to describe this case, which we anticipate would lead to minor numerical changes in the coefficients of the terms in the fluid equations if the analysis is carried through in the same way.

[1] A. Cohen, D. Kaplan, and A. Nelson, Nucl. Phys. **B373**, 453 (1992); Phys. Lett. B **294**, 57 (1992).
[2] M. Joyce, T. Prokopec, and N. Turok, Phys. Lett. B **338**, 269 (1994).
[3] K. Funakubo, A. Kakuto, S. Otsuki, K. Takenaga, and F. Toyoda, Phys. Rev. D **50**, 1105 (1994); in *Proceedings of the 27th International Conference on High Energy Physics*, Glasgow, Scotland, 1994, edited by P. J. Bussey and I. G. Knowles (IOP, London, 1995); Prog. Theor. Phys. **93**, 1067 (1995).
[4] M. Joyce, T. Prokopec, and N. Turok, Phys. Rev. Lett. **75**, 1695 (1995).
[5] N. Turok, Phys. Rev. Lett. **68**, 1803 (1992); M. Dine, R. Leigh, P. Huet, A. Linde, and D. Linde, Phys. Rev. D **46**, 550 (1992); B.-H. Liu, L. McLerran, and N. Turok, *ibid.* **46**, 2668 (1992); T. Prokopec and G. Moore, Phys. Rev. Lett. **75**, 777 (1995); G. Moore and T. Prokopec, Phys. Rev. D **52**, 7182 (1995).
[6] M. Joyce, T. Prokopec, and N. Turok, preceding paper, Phys. Rev. D **53**, 2930 (1996).
[7] S. Nasser and N. Turok, Princeton Report No. PUPT-1456, 1994 (unpublished).
[8] A. Cohen, D. Kaplan, and A. Nelson, Phys. Lett. B **263**, 86 (1991).
[9] M. Dine and S. Thomas, Phys. Lett. B **328**, 73 (1994).
[10] M. Joyce, T. Prokopec, and N. Turok, Phys. Lett. B **393**, 312 (1994).
[11] M. Joyce, in *Electroweak Physics and the Early Universe*, Proceedings of the Sintra Conference, 1994, edited by J. Romao and F. Freire (Plenum, New York, 1994).
[12] A. Cohen, D. Kaplan, and A. Nelson, Phys. Lett. B **336**, 41 (1994).
[13] S. Nasser and N. Turok (unpublished).
[14] G. F. Guidice and M. Shaposhnikov, Phys. Lett B **326**, 118 (1994).
[15] P. Huet and A. E. Nelson, Phys. Lett. B **355**, 229 (1995); Phys. Rev. D (to be published); A. Riotto, Report No. hep-ph/9510271 (unpublished).
[16] L. McLerran, M. Shaposhnikov, N. Turok, and M. Voloshin, Phys. Lett. B **256**, 451 (1991).
[17] D. Comelli, M. Pietroni, and A. Riotto, Phys. Rev. D (to be published); Phys. Lett. B **354**, 91 (1995), and references therein.
[18] H. E. Haber, in *Spin Structure in High Energy Processes*, Proceedings of the 21st SLAC Summer Institute on Particle Physics, Stanford, California, 1993, edited by L. DePorcel and C. Dunwoodie (SLAC Report No. 444, Stanford, 1994).